Honda, S., Kagoshima, M., Wanaka, A., Tohyama, M., Matsumoto, K., Nakamura, T., 1995. Localization and functional coupling of HGF and c-Met/HGF receptor in rat brain: implication as neurotrophic factor. Brain Res. Mol. Brain Res. 32, 197–210.

Ilzecka, J., Stelmasiak, Z., Dobosz, B., 2001. Interleukin-1ß converting enzyme/Caspase-1 (ICE/Caspase-1) and soluble APO-1/Fas/CD 95 receptor in amyotrophic lateral sclerosis patients. Acta Neurol. Scand. 103, 255–258.

Imai, Y., Ibata, I., Ito, D., Ohsawa, K., Kohsaka, S., 1996. A novel gene iba1 in the major histocompatibility complex class III region encoding an EF hand protein expressed in a monocytic lineage. Biochem. Biophys. Res. Commun. 224, 855–862.

Inoue, H., Tsukita, K., Iwasato, T., Suzuki, Y., Tomioka, M., Tateno, M., Nagao, M., Kawata, A., Saido, T.C., Miura, M., Misawa, H., Itohara, S., Takahashi, R., 2003. The crucial role of caspase-9 in the disease progression of a transgenic ALS mouse model. EMBO J. 22, 6665–6674.

Jiang, Y.M., Yamamoto, M., Kobayashi, Y., Yoshihara, T., Liang, Y., Terao, S., Takeuchi, H., Ishigaki, S., Katsuno, M., Adachi, H., Niwa, J., Tanaka, F., Doyu, M., Yoshida, M., Hashizume, Y., Sobue, G., 2005. Gene expression profile of spinal motor neurons in sporadic amyotrophic lateral sclerosis. Ann. Neurol. 57, 236–251.

John, G.R., Chen, L., Rivieccio, M.A., Melendez-Vasquez, C.V., Hartley, A., Brosnan, C.F., 2004. Interleukin-1ß induces a reactive astroglial phenotype via deactivation of the Rho GTPase-Rock axis. J. Neurosci. 24, 2837–2845.

Kaspar, B.K., Llado, J., Sherkat, N., Rothstein, J.D., Gage, F.H., 2003. Retrograde viral delivery of IGF-1 prolongs survival in a mouse ALS model. Science 301, 839–842.

Kato, S., Funakoshi, H., Nakamura, T., Kato, M., Nakano, I., Hirano, A., Ohama, E., 2003. Expression of hepatocyte growth factor and c-Met in the anterior horn cells of the spinal cord in the patients with amyotrophic lateral sclerosis (ALS): immunohistochemical studies on sporadic ALS and familial ALS with superoxide dismutase 1 gene mutation. Acta Neuropathol. 106, 112–120.

Keep, M., Elmer, E., Fong, K.S., Csiszar, K., 2001. Intrathecal cyclosporin prolongs survival of late-stage ALS mice. Brain Res. 894, 327–331.

Kostic, V., Jackson-Lewis, V., de Bilbao, F., Dubois-Dauphin, M., Przedborski, S., 1997. Bcl-2: prolonging life in a transgenic mouse model of familial amyotrophic lateral sclerosis. Science 277, 559–562.

Kriz, J., Nguyen, M.D., Julien, J.P., 2002. Minocycline slows disease progression in a mouse model of amyotrophic lateral sclerosis. Neurobiol. Dis. 10, 268–278.

Li, M., Ona, V.O., Guegan, C., Chen, M., Jackson-Lewis, V., Andrews, L.J., Olszewski, A.J., Stieg, P.E., Lee, J.P., Przedborski, S., Friedlander, R.M., 2000. Functional role of caspase-1 and caspase-3 in an ALS transgenic mouse model. Science 288, 335–339.

Meeuwsen, S., Persoon-Deen, C., Bsibsi, M., Ravid, R., van Noort, J.M., 2003. Cytokine, chemokine and growth factor gene profiling of cultured human astrocytes after exposure to proinflammatory stimuli. Glia 43, 243–253.

Morizane, Y., Honda, R., Fukami, K., Yasuda, H., 2005. X-linked inhibitor of apoptosis functions as ubiquitin ligase toward mature caspase-9 and cytosolic Smac/DIABLO. J. Biochem. (Tokyo) 137, 125–132.

Nagai, M., Re, D.B., Nagata, T., Chalazonitis, A., Jessell, T.M., Wichterle, H., Przedorski, S., 2007. Astrocytes expressing ALS-linked mutated SOD1 release factors selectively toxic to motor neurons. Nat. Neurosci. 10, 615–622.

Nakamura, T., Nawa, K., Ichihara, A., 1984. Partial purification and characterization of hepatocyte growth factor from serum of hepatectomized rats. Biochem. Biophys. Res. Commun. 122, 1450–1459.

Nakamura, T., Nishizawa, T., Hagiya, M., Seki, T., Shimonishi, M., Sugimura, A., Tashiro, K., Shimizu, S., 1989. Molecular cloning and expression of human hepatocyte growth factor. Nature 342, 440–443.

Novak, K.D., Prevette, D., Wang, S., Gould, T.W., Oppenheim, R.W., 2000. Hepatocyte growth factor/scatter factor is a neurotrophic survival factor for lumbar but not for other somatic motor neurons in the chick embryo. J. Neurosci. 20, 326–337.

Pasinelli, P., Houseweart, M.K., Brown Jr., R.H., Cleveland, D.W., 2000. Caspase-1 and -3 are sequentially activated in motor neuron death in Cu, Zn superoxide dismutase-mediated familial amyotrophic lateral sclerosis. Proc. Natl. Acad. Sci. U.S.A. 97, 13901–13906.

Pasinelli, P., Brown Jr., R.H., 2006. Molecular biology of amyotrophic lateral sclerosis: insights from genetics. Nat. Rev. Neurosci. 7, 710–723.

Sakamoto, T., Kawazoe, Y., Shen, J.S., Takeda, Y., Arakawa, Y., Ogawa, J., Oyanagi, K., Ohashi, T., Watanabe, K., Inoue, K., Eto, Y., Watabe, K., 2003. Adenoviral gene transfer of GDNF, BDNF and TGF beta 2, but not CNTF, cardiotrophin-1 or IGF1, protects injured adult motor neurons after facial nerve avulsion. J. Neurosci. Res. 72, 54–64.

Sendtner, M., Holtmann, B., Kolbeck, R., Thoenen, H., Barde, Y.A., 1992. Brain-derived neurotrophic factor prevents the death of motor neurons in newborn rats after nerve section. Nature 360, 757–759.

Shi, Y., 2004. Caspase activation, inhibition, and reactivation: a mechanistic view. Protein Sci. 13, 1979–1987.

Sun, W., Funakoshi, H., Nakamura, T., 2002. Overexpression of HGF retards disease progression and prolongs life span in a transgenic mouse model of ALS. J. Neurosci. 22, 6537–6548.

Thornberry, N.A., Bull, H.G., Calaycay, J.R., Chapman, K.T., Howard, A.D., Kostura, M.J., Miller, D.K., Molineaux, S.M., Weidner, J.R., Aunins, J., Elliston, K.O., Ayala, J.M., Casano, F.J., Chin, J., Ding, G.J.F., Egger, L.A., Gaffney, E.P., Limjuco, G., Palyha, O.C., Raju, S.M., Rolando, A.M., Salley, J.P., Yamin, T.-T., Lee, T.D., Shively, J.E., MacCross, M., Mumford, R.A., Schmidt, J.A., Tocci, M.J., 1992. A novel heterodimeric cysteine protease is required for interleukin-1ß processing in monocytes. Nature 356, 768–774.

Van Den Bosch, L., Tilkin, P., Lemmens, G., Robberecht, W., 2002. Minocycline delays disease onset and mortality in a transgenic model of ALS. Neuroreport 13, 1067–1070.

Wang, L.J., Lu, Y.Y., Muramatsu, S., Ikeguchi, K., Fujimoto, K., Okada, T., Mizukami, H., Matsushita, T., Hanazono, Y., Kume, A., Nagatsu, T., Ozawa, K., Nakano, I., 2002. Neuroprotective effects of glial cell line-derived neurotrophic factor mediated by an adeno-associated virus vector in a transgenic animal model of amyotrophic lateral sclerosis. J. Neurosci. 22, 6920–6928.

Weydt, P., Yuen, E.C., Ransom, B.R., Moller, T., 2004. Increased cytotoxic potential of microglia from ALS-transgenic mice. GLIA 48, 179–182.

Xiao, Q., Zhao, W., Beers, D.R., Yen, A.A., Xie, W., Henkel, J.S., Appel, S.H., 2007. Mutant SOD1G93A microglia are more neurotoxic relative to wild-type microglia. J. Neurochem. 102, 2008–2019.

Yamamoto, Y., Livet, J., Pollock, R.A., Garces, A., Arce, V., deLapeyriere, O., Henderson, C.E., 1997. Hepatocyte growth factor (HGF/SF) is a muscle-derived survival factor for a subpopulation of embryonic motor neurons. Development 124, 2903–2913.

Yrjanheikki, J., Tikka, T., Keinanen, R., Goldsteins, G., Chan, P.H., Koistinaho, J., 1999. A tetracycline derivative, minocycline, reduces inflammation and protects against focal cerebral ischemia with a wide therapeutic window. Proc. Natl. Acad. Sci. U.S.A. 96, 13496–13500.

Zhu, S., Stavrovskaya, I.G., Drozda, M., Kim, B.Y., Ona, V., Li, M., Sarang, S., Liu, A.S., Hartley, D.M., Wu, D.C., Gullans, S., Ferrante, R.J., Przedborski, S., Kristal, B.S., Friedlander, R.M., 2002. Minocycline inhibits cytochrome *c* release and delays progression of amyotrophic lateral sclerosis in mice. Nature 417, 74–78.

J Neuropathol Exp Neurol

Vol. 66, No. 11
November 2007
pp. 1037–1044

ORIGINAL ARTICLE

Intrathecal Delivery of Hepatocyte Growth Factor From Amyotrophic Lateral Sclerosis Onset Suppresses Disease Progression in Rat Amyotrophic Lateral Sclerosis Model

Aya Ishigaki, MD, PhD, Masashi Aoki, MD, PhD, Makiko Nagai, MD, PhD, Hitoshi Warita, MD, PhD, Shinsuke Kato, MD, PhD, Masako Kato, MD, PhD, Toshikazu Nakamura, PhD, Hiroshi Funakoshi, MD, PhD, and Yasuto Itoyama, MD, PhD

Abstract

Hepatocyte growth factor (HGF) is one of the most potent survival-promoting factors for motor neurons. We showed that introduction of the HGF gene into neurons of G93A transgenic mice attenuates motor neuron degeneration and increases the lifespan of these mice. Currently, treatment regimens using recombinant protein are closer to clinical application than gene therapy. To examine its protective effect on motor neurons and therapeutic potential we administered human recombinant HGF (hrHGF) by continuous intrathecal delivery to G93A transgenic rats at doses of 40 or 200 μg and 200 μg at 100 days of age (the age at which pathologic changes of the spinal cord appear, but animals show no clinical weakness) and at 115 days (onset of paralysis), respectively, for 4 weeks each. Intrathecal administration of hrHGF attenuates motor neuron degeneration and prolonged the duration of the disease by 63%, even with administration from the onset of paralysis. Our results indicated the therapeutic efficacy of continuous intrathecal administration of hrHGF in transgenic rats and should lead to the consideration for further clinical trials in amyotrophic lateral sclerosis using continuous intrathecal administration of hrHGF.

Key Words: Amyotrophic lateral sclerosis, Continuous intrathecal delivery, Hepatocyte growth factor, Neurodegeneration, Superoxide dismutase-1 (SOD1), Transgenic rat.

From the Department of Neurology (AI, MA, MN, HW, YI), Tohoku University Graduate School of Medicine, Sendai, Japan; Tohoku University Hospital ALS Center (AI, MA, HW, YI), Sendai, Japan; Department of Neuropathology (SK), Institute of Neurological Sciences, Faculty of Medicine Tottori University, Yonago, Japan; Division of Pathology (MK), Tottori University Hospital, Yonago, Japan; and Division of Molecular Regenerative Medicine (TN, HF), Department of Biochemistry and Molecular Biology, Osaka University Graduate School of Medicine, Osaka, Japan.

Send correspondence and reprint requests to: Masashi Aoki, MD, PhD, Department of Neurology, Tohoku University Graduate School of Medicine, 1-1 Seiryo-machi, Sendai 980-8574, Japan; E-mail: aokim@mail.tains.tohoku.ac.jp

This work was supported by a grant from the Ministry of Health, Labor, and Welfare, Japan (YI, MA, SK, HF). Research funding was also provided by the Haruki ALS Research Foundation (YI, MA, HW) and by a Grant-in-Aid for Scientific Research from the Ministry of Education, Culture, Sports, Science, and Technology, Japan (MA, SK, HF).

INTRODUCTION

Amyotrophic lateral sclerosis (ALS) is a fatal neurodegenerative disease caused by selective motor neuron death (1). Approximately 10% of cases of ALS are inherited, usually as an autosomal dominant trait (2). In ~25% of familial cases, the disease is caused by mutations in the gene encoding cytosolic copper-zinc superoxide dismutase (SOD1) (3–5). The cause of ALS is still unclear, and clinical trials have as yet failed to identify any truly effective therapeutic regimens for ALS, with only riluzole providing a modest improvement in survival. Various substances have been shown to have therapeutic effects in a murine model of ALS. However, there have been a few reports of prolongation of survival with treatment starting around the time of disease onset (6–12).

We (13) and another group (14) developed a rat model of ALS expressing a human SOD1 transgene with 2 ALS-associated mutations: glycine to alanine at position 93 (G93A) and histidine to arginine at position 46 (H46R) (3, 5). Similar to its murine counterpart, this rat transgenic (Tg) ALS model reproduces the major phenotypic features of human ALS. Some experimental manipulations are difficult in Tg mice because of size limitations; however, this Tg rat model allows routine implantation of infusion pumps for intrathecal drug delivery. Intrathecal drug application is a well-established method for therapy and has been used in clinical trials in patients with ALS (15). This route of administration bypasses the blood-brain barrier, allowing rapid access to potential binding sites for the test compound in the spinal cord (16).

Hepatocyte growth factor (HGF) was first identified as a potent mitogen for mature hepatocytes and was first cloned in 1989 (17). Detailed studies indicated that HGF is expressed in the CNS (18) and is a novel neurotrophic factor (19, 20). HGF is one of the most potent survival-promoting factors for motor neurons, comparable to glial cell line-derived neurotrophic factor in vitro (21). Sun et al (22) reported that introduction of the HGF gene into neurons of G93A Tg mice attenuates motor neuron degeneration and increases the lifespan of these mice. Thus, HGF is a good candidate agent for treatment of ALS. Currently, treatment using recombinant protein is closer to clinical application than gene therapy. However, HGF has a very

short half-life (23–25) and shows poor penetration into the CNS. Therefore, we examined the effects of continuous intrathecal delivery of human recombinant HGF (hrHGF) into Tg rats using implanted infusion pumps for selective and less invasive supply of HGF to the spinal cord.

MATERIALS AND METHODS

Animal Preparation and Clinical Evaluation

G93A Tg rats were genotyped by polymerase chain reaction (PCR) assay using DNA obtained from the tail as described (13). To examine the dose and effects of hrHGF on disease onset, we began administration of 40 or 200 μg of hrHGF (provided by H. Funakoshi and T. Nakamura, Osaka University, Osaka, Japan) or vehicle (0.1 M sulfoxide PBS) for 4 weeks to groups of eight 100-day-old Tg rats, when the pathologic changes of the spinal cord appeared, but the animals did not show weakness. All animals were killed at 130 days by deep anesthesia, and the spinal cords were examined. Because treatment of patients with ALS patients is initiated only after diagnosis based on clinical signs and symptoms, we tested the effects of hrHGF on survival with administration beginning at around the age of onset of paralysis. We administered 200 μg of hrHGF or vehicle alone to groups of eight 115-day-old G93A Tg rats for 4 weeks, and the animals were observed until their death. To analyze the mechanism of action of hrHGF administration beginning at onset of paralysis we treated groups of six 115-day-old G93A Tg rats with 100 μg of hrHGF or with vehicle alone for 2 weeks (a dose comparable to 200 μg for 4 weeks). All rats were killed 2 weeks after commencement of administration of hrHGF, and their lumbar spinal cords were examined. Further groups of 3 G93A Tg rats and 3 non-Tg rats at 70, 100, and 130 days were used to measure the levels of rat HGF and c-Met. All rats were handled according to approved animal protocols of our institution and had free access to food and water throughout the experimental period and before and after pump implantation.

The onset of ALS was scored as the first observation of abnormal gait, evidence of limb weakness, or loss of extension of the hindlimbs when picked up at the base of the tail. We defined the appearance of paralysis as disease onset, although this is not a sensitive indicator and appears later than the decrease in activity (10). However, the appearance of paralysis is a suitable marker of disease onset because it is closer to the state at which patients will be diagnosed with the disease.

Footprints were collected every 3 days by letting the rats walk on a straight path after dipping their hind paws in black ink. We measured 3 strides within the area showing regular gait and calculated the means. Footprint measurements were made for rats that began treatment at 115 days. Examiners were blinded to which group each of the rats belonged in.

Preparation of the Osmotic Pumps and Transplant Surgery

Osmotic pumps (model number 2004 or 2002; Durect Corporation, Cupertino, CA) were incubated in sterile saline at 37°C for 40 hours to attain a constant flow rate before use. Pumps were filled to capacity with hrHGF solution or vehicle using a filling needle. An infusion tube was made by connecting a 1-cm length of polyethylene tubing (PE 60; Becton Dickinson, Franklin Lakes, NJ) to a small caliber tube 9 cm in length (PE 10; Becton Dickinson) using an adhesive (ARON ALPHA; Konishi Co., Osaka, Japan). The end of the infusion tube was connected to the shorter end of the flow moderator, the longer end of which was inserted into the pump.

Surgery for placement of the pump and intrathecal administration was performed as follows. Tg rats were anesthetized using diethyl ether and 1% halothane in a mixture of 30% oxygen and 70% nitrous oxide. The skin over the third to fifth lumbar spinal process was incised and the paravertebral muscles were separated from the vertebral lamina with scissors. The fifth lumbar vertebra was laminectomized, and the dura mater was exposed for insertion of the infusion tube. Particular care was taken not

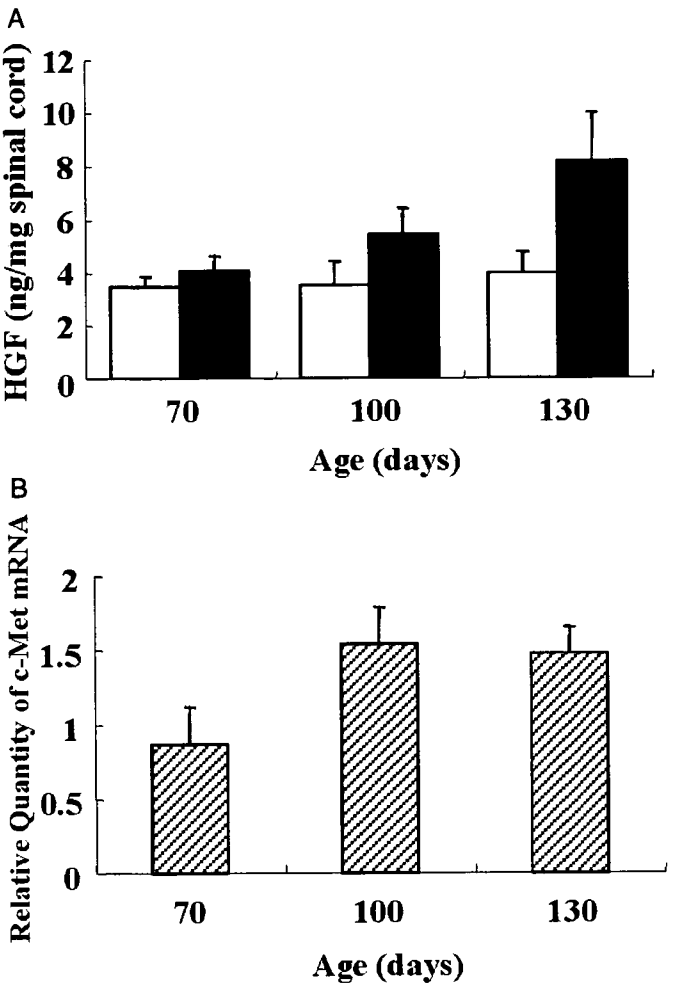

FIGURE 1. Increased levels of rat hepatocyte growth factor (HGF) and c-Met expression in the spinal cords of G93A transgenic (Tg) rats (n = 3) and non-Tg rats (n = 3). **(A)** Levels of endogenous rat HGF expression. Open bars, non-Tg rats; closed bars, G93A Tg rats. **(B)** Levels of c-Met mRNA of G93A Tg rats compared with non-Tg rats.

to injure the dura mater during laminectomy. A small hole was bored through the dura mater with a 24-gauge needle, and a polyethylene tube (PE 10, Becton Dickinson) was inserted into the subarachnoid space approximately 3 cm rostrally. A subcutaneous pocket was made into which the osmotic pump and pump side tube were implanted. The infusion tube was attached to the fascia over the paravertebral muscles at the incision margin with silk string. A drop of adhesive (ARON ALPHA) was applied, and the incision was closed by suturing the muscles and skin.

Measurement of Rat and Human HGF in the Lumbar Spinal Cord

Slices of the fifth lumbar cord from 3 G93A Tg rats and 3 non-Tg rats at 70, 100, and 130 days as well as from 130-day-old G93A Tg rats treated with 40 or 200 μg of hrHGF or vehicle alone for 4 weeks starting at 100 days were homogenized in buffer (20 mM Tris-HCl, pH 7.5, 0.1% Tween-80, 1 mM phenylmethylsulfonyl fluoride, and 1 mM EDTA) and centrifuged at 15,000 rpm for 30 minutes. Supernatants were separated and the concentrations of rat endogenous HGF were measured using an enzyme-linked immunosorbent assay (ELISA) kit, which is specific for rat HGF without detecting human HGF (22) (Institute of Immunology, Tokyo, Japan). For measurement of human HGF in the treated rats we used a human HGF-specific ELISA kit (IMMUNIS, Institute of Immunology), which is not reactive with rat HGF (26, 27).

Measurement of c-Met mRNA in the Lumbar Spinal Cord of Tg Rats

Aliquots of 1 μg of total RNA from the lumbar cords of rats were used as templates for synthesis of double-stranded cDNA. Real-time quantitative PCR was performed for c-Met and glyceraldehyde-3-phosphate dehydrogenase (GAPDH) [GAPDH forward primer, 5′-CCATCACTGCCACTCAGAAGAC-3′; GAPDH reverse primer, 5′-TCATACTTGGCAGGTTTCTCCA-3′; GAPDH TaqMan probe, 5′(FAM)-ACCACGAGCACTGTTTCAATAGGACCC-(TAMRA)3′; c-MET forward primer, 5′-GTACGGTGTCTCCAGCATTTTT-3′; c-Met reverse primer, 5′-AGAGCACCACCTGCATGAAG-3′; TaqMan probe, 5′(FAM)-CGTGTTCCTACCCCCAATGTATCCGT- (TAMRA)3′]. An ABI Prism 7700 Sequence Detection System (Applied Biosystems Perkin-Elmer, Foster City, CA) was used to monitor emission intensities using the above primer pairs and TaqMan fluorogenic probes. The c-Met mRNA level of G93A Tg rats relative to non-Tg rats was calculated using the Comparative C_T Method (Applied Biosystems).

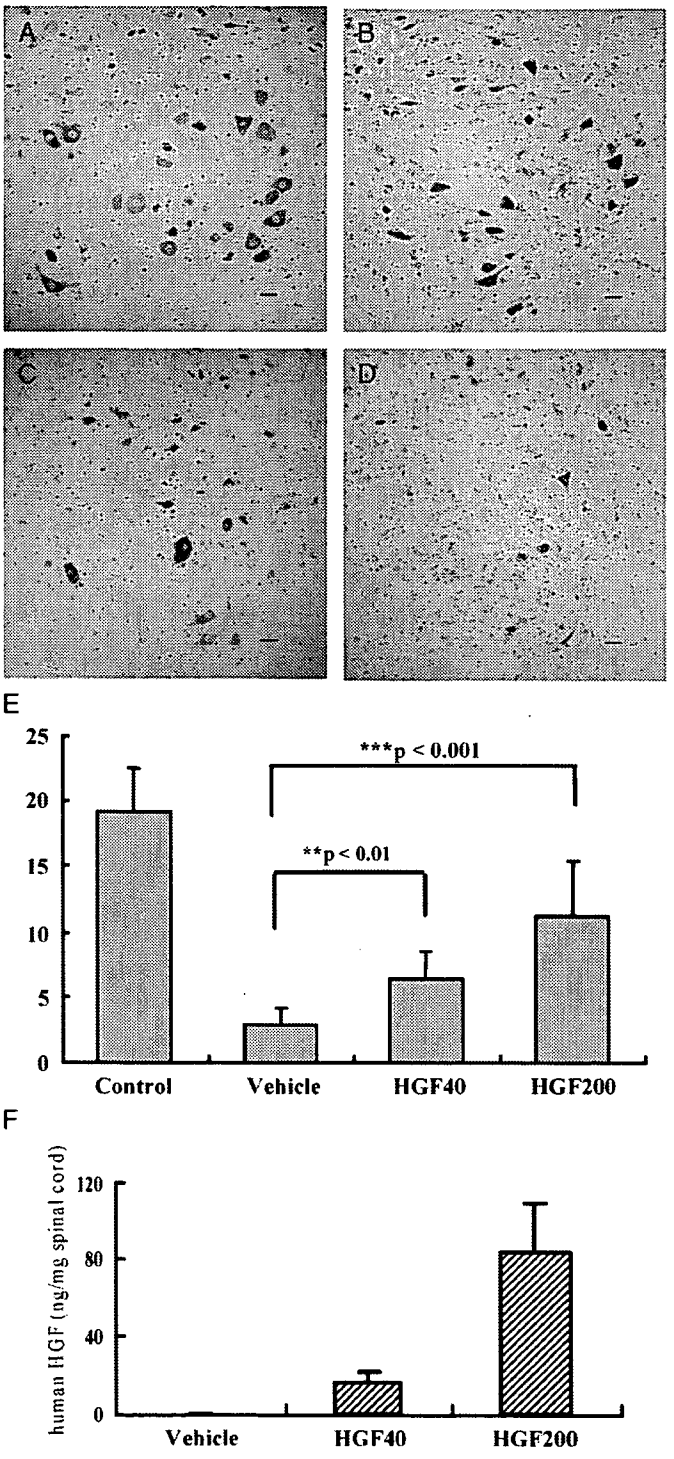

FIGURE 2. Intrathecal administration of hepatocyte growth factor (HGF) to G93A transgenic (Tg) rats at 100 days showed a protective effect against motor neuron death. **(A–D)** Histologic evaluation of the anterior horn with Nissl staining at 130 days: **(A)** lumbar cord of non-Tg rats; **(B)** 200 μg of human recombinant HGF (hrHGF)-treated; **(C)** 40 μg of hrHGF-treated; and **(D)** vehicle-treated G93A Tg rats. Scale bar = 40 μm. **(E)** Quantitative morphometric evaluation of surviving motor neurons of the fifth lumbar anterior horn at 130 days. We counted neurons that were >40 μm in diameter. Significantly larger numbers of motor neurons survived in hrHGF-treated G93A Tg rats ($p < 0.01$ and $p < 0.001$, 40 and 200 μg of hrHGF, respectively), compared with vehicle-treated G93A Tg rats (n = 8 in each group). **(F)** Levels of human HGF concentration in lumbar spinal cords of G93A Tg rats treated with 200 μg of hrHGF, 40 μg of hrHGF, and vehicle.

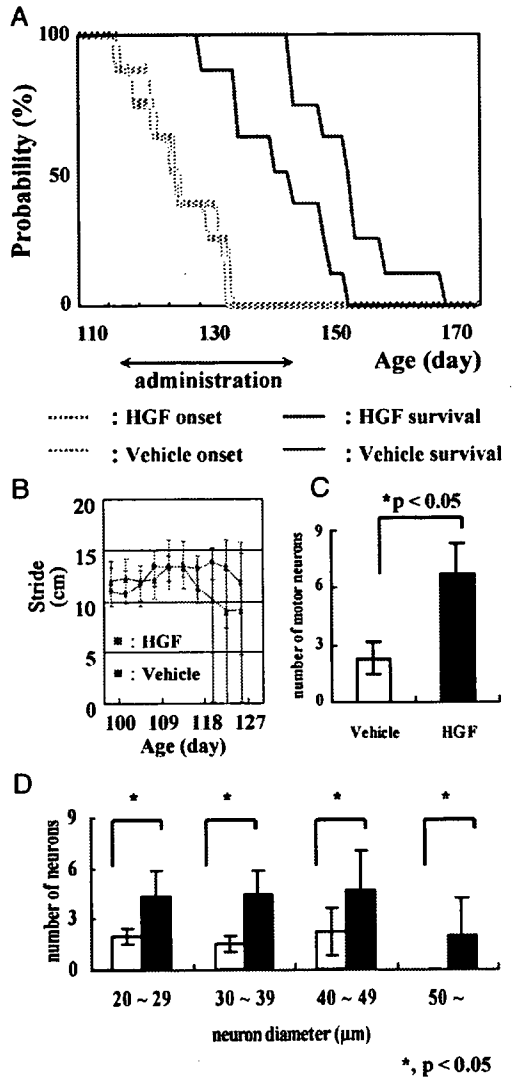

FIGURE 3. Intrathecal administration of hepatocyte growth factor (HGF) from 115 days (just before disease onset) retarded disease progression. **(A)** Survival periods were 143.25 ± 17.0 days in the vehicle-treated group (solid blue line) and 154.3 ± 16.4 days in the 200 μg of human recombinant HGF (hrHGF)-treated group (solid red line). Survival of hrHGF-treated animals was extended significantly ($p = 0.0135$), although there were no significant differences in onset (dotted lines, $n = 8$ in each group, $p = 0.6346$). **(B)** Footprint analysis demonstrated a delay in decline of stride length in G93A transgenic (Tg) rats treated with 200 μg of hrHGF relative to vehicle-treated G93A Tg rats (error bars, ± SD). **(C, D)** Quantitative morphometric evaluation of surviving motor neurons that were >40 μm in diameter **(C)** and neuron size distribution **(D)** in the fifth lumbar anterior horn of G93A Tg rats 2 weeks after administration from 115 days. Significantly larger number of motor neurons survived in the hrHGF-treated G93A Tg rats compared with vehicle-treated G93A Tg rats (6.7 ± 1.6 vs 2.3 ± 0.9; $p = 0.002$, $n = 6$ in each group) **(C)**.

Histopathologic and Immunohistochemical Analyses

To examine the dose and effects of hrHGF against disease onset, we began administration of 40 or 200 μg of hrHGF or vehicle alone to groups of eight 100-day-old Tg rats each for 4 weeks. At 130 days, G93A Tg rats were administered hrHGF or vehicle, and non-Tg rats were deeply anesthetized with diethyl ether and killed for histopathologic evaluation. To examine the effects of hrHGF administration beginning at onset of paralysis, 100 μg of HGF or vehicle alone was administered to groups of six 115-day-old Tg rats for 2 weeks. These animals were killed by deep anesthesia with diethyl ether 2 weeks after the operation. Under deep anesthesia these animals were perfused via the aorta with physiologic saline at 37°C and their lumbar spinal cords were removed. The fifth lumbar spinal cord tissue was embedded in OCT compound (Sakura Finetek Japan Co., Tokyo, Japan), frozen in an acetone/dry ice bath after fixation with 4% paraformaldehyde, and supplemented with 0.1 M cacodylate buffer (pH 7.3) containing 30% sucrose. Other spinal cord tissue specimens were frozen in dry ice and cut into frozen sections (12-μm-thick) and then washed with PBS. To evaluate the effects of HGF on motor neuron loss we compared the numbers of lumbar motor neurons in each group by counting as mentioned below. To evaluate the effects of HGF on apoptosis and to determine whether HGF receptors were activated, we compared the results of immunohistochemical staining of the lumbar cords for activated caspase-3, activated caspase-9 (Cell Signaling Technology, Inc., Beverly, MA), and phosphorylated c-Met (activated HGF receptor) (BioSource International, Camerillo, CA). The staining specificity of the antibodies was assessed by preabsorption of the primary antibody with excess peptide, omission of the primary antibody, or replacement of the primary antibody with normal rabbit IgG (22). We examined every seventh section from 42 serial sections of the fifth lumbar spinal cord. We counted neurons that had a clear nucleolus and were multipolar with neuronal morphology (13, 22), >40 μm in diameter, and located in a defined area of the anterior horn of the spinal cord. Cell counts were performed using ImageJ software (National Institutes of Health, Bethesda, MD) on images captured electronically (28).

Western Blotting

Lysates from the lumbar spinal cord of each rat were prepared in RIPA buffer (150 mM NaCl, 1% Nonidet P-40, 0.5% deoxycholate, 0.1% sodium dodecyl sulfate, and 50 mM Tris, pH 8.0). Equal amounts of proteins from the lysates (50 μg) were resolved by sodium dodecyl sulfate-polyacrylamide gel electrophoresis, transferred onto polyvinylidene diflouride membranes, and immunoblotted. The primary antibodies used were anti-caspase-3 (Sigma-Aldrich, St. Louis, MO), anti-caspase-9 (Stressgen Biotechnologies Corporation, Victoria, BC, Canada), anti-X-linked inhibitor of apoptosis protein (XIAP) (Cell Signaling Technology, Inc.), and anti-excitatory amino acid transporter 2 (EAAT2) antibodies (Chemicon International, Temecula, CA). After incubation of membranes with HRP-coupled

secondary antibodies, proteins were visualized using ECL or ECL Plus Western Blotting Detection Reagents (Amersham Biosciences Inc., Piscataway, NJ) and a Fluorochem image analyzer (LAS-3000 mini; Fuji Photo Film Co., Tokyo, Japan).

Statistical Analysis

The Kaplan-Meier and log-rank test were used for statistical analyses of differences in onset and survival between groups. For statistical analyses of differences in body weight, footprint, motor neuron cell count, and Western blotting we used analysis of variance and post hoc tests. The data are reported as means ± SD.

RESULTS

Measurement of the Levels of Rat HGF and c-Met Expression in Untreated Animals

Groups of 3 G93A Tg rats and non-Tg rats at 70, 100, and 130 days were used to measure the levels of rat HGF without any treatment. In the lumbar cords of untreated G93A Tg rats, the HGF concentrations increased with disease progression (Fig. 1A). At 70 days the level of rat HGF in the lumbar cords of G93A Tg rats was 4.05 ± 0.6 ng/mg and was the same as that of non-Tg rats. Increases of 35% and 107% were observed in the rat HGF level at 100 and 130 days, respectively, compared with non-Tg rats.

In addition, we measured the levels of c-Met mRNA in the lumbar spinal cords of Tg rats relative to non-Tg rats by real-time quantitative PCR. In the lumbar cords of G93A Tg rats the level of c-Met mRNA expression was the same as that in non-Tg rats at 70 days. However, a 55% increase in the level of c-Met mRNA expression compared with that of non-Tg rats was observed at 100 days and the higher level of expression was retained at 130 days (Fig. 1B).

Administration of hrHGF to 100-Day-Old G93A Tg Rats for 4 Weeks

To examine the efficacy of hrHGF on motor neurons in the spinal cords of Tg rats against onset of disease we administered 40 and 200 μg of hrHGF or vehicle alone to 100-day-old G93A Tg rats for 4 weeks (n = 8 in each group). Animals were killed at 130 days, and their lumbar spinal cords were examined. Because administration of hrHGF for more than 30 days may induce antibodies against hrHGF, we did not treat rats for longer than this period. We confirmed elevation of human HGF concentrations in the lumbar cords of hrHGF-treated rats using a specific sandwich immunoassay. The mean human HGF concentrations were 83.9 ± 25.1, 15.6 ± 5.4, and 0 ng/mg for rats treated with 200 μg of hrHGF, 40 μg of hrHGF, and vehicle, respectively (Fig. 2F). The endogenous rat HGF concentration is 4 to 5 ng/mg at this age (Fig. 1A). The human HGF concentration in the spinal cord of G93A Tg rats treated with 200 μg of hrHGF

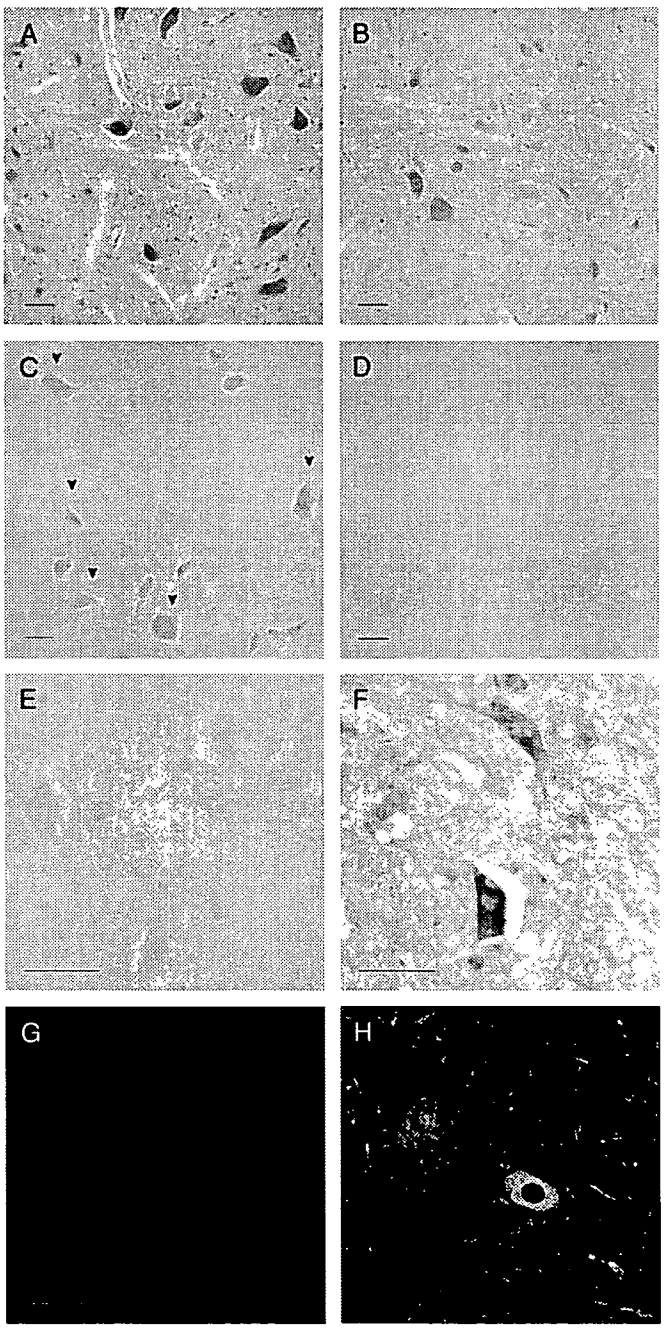

FIGURE 4. Sections of the fifth lumbar anterior horn from G93A transgenic (Tg) rats treated with human recombinant hepatocyte growth factor (hrHGF) **(A, C, E, G)** or vehicle **(B, D, F, H)** for 2 weeks starting at 115 days were stained with hematoxylin and eosin **(A, B)** and antibodies to phosphorylated c-Met **(C, D)**, activated caspase-3 **(E, F)**, and activated caspase-9 **(G, H)**. Scale bar = 50 μm. There were larger numbers of remaining large motor neurons in hrHGF-treated G93A Tg rats (6.7 ± 1.6) **(A)** than in vehicle-treated G93A Tg rats (2.3 ± 0.9) **(B)**. Phosphorylated c-Met staining was more distinct in hrHGF-treated G93A Tg rats **(C)** than in vehicle-treated G93A Tg rats **(D)**. In contrast, activated caspase-3 staining was stronger in vehicle-treated G93A Tg rats **(F)** than in hrHGF-treated G93A Tg rats **(E)**. Activated caspase-9 staining was detectable in vehicle-treated G93A Tg rats **(H)** compared with little reactivity in hrHGF-treated G93A Tg rats **(G)**.

was increased by approximately 20-fold relative to the endogenous rat HGF. All vehicle-treated G93A Tg rats developed weakness in the hindlimbs with a mean onset of 118.8 ± 4.3 days. Seven of 8 G93A Tg rats treated with 40 μg of rhHGF developed the disease before 130 days. In contrast, only 3 of 8 animals treated with 200 μg of rhHGF developed paralysis before this stage. At 130 days the average numbers of motor neurons in the ventral horn were as follows: non-Tg rats, 19.2 ± 3.3; vehicle only, 2.9 ± 1.3; 40 μg of hrHGF, 6.3 ± 2.1; and 200 μg of hrHGF, 11.2 ± 4.2. Significantly more motor neurons survived in hrHGF-treated (40 μg, $p < 0.01$; 200 μg, $p < 0.001$) than in vehicle-treated G93A Tg rats (Fig. 2A–E). hrHGF prevented motor neuron death in G93A Tg rats in a dose-dependent manner.

Administration of hrHGF to 115-Day-Old G93A Tg Rats for 4 Weeks

We next examined the therapeutic potential of HGF when administration was started at around the age of onset of paralysis. We administered 200 μg of hrHGF or vehicle alone to 115-day-old G93A Tg rats for 4 weeks. There were no statistically significant differences ($p = 0.6346$) in onset between the groups (200 μg of hrHGF, 126.8 ± 13.1 days; vehicle, 126.3 ± 13.8 days) (Fig. 3A, dotted lines). In contrast, 200 μg of hrHGF extended mean survival by 11 days compared with vehicle-treated G93A Tg rats ($p = 0.0135$) (Fig. 3A, solid lines), although G93A Tg rats showed very rapid disease progression and died within 20 days of disease onset. The average periods from the onset to death were 16.9 ± 8.17 and 27.5 ± 11.1 days in vehicle ($n = 8$) and hrHGF ($n = 8$) groups, respectively. The latter represented an increase of 62.7% relative to vehicle-treated controls. Footprint analysis of stride length in 200 μg of hrHGF-treated G93A Tg rats showed significant improvement compared with vehicle-treated G93A Tg rats at 118 days ($p = 0.0424$) (Fig. 3B). Thus, despite the very rapid disease progression in this model and short treatment period of 4 weeks, hrHGF treatment improved motor performance and prolonged survival even with treatment beginning around the onset of paralysis.

Histologic evaluation of the lumbar spinal cord indicated that hrHGF treatment prevented the pathologic changes typical of Tg rats. Two weeks after commencement of administration at 129 days, vehicle-treated rats showed substantial loss of motor neurons (2.3 ± 0.9) compared with hrHGF-treated rats (6.6 ± 1.6) (Figs. 3C, 4A, B). A significantly larger number of motor neurons survived in hrHGF-treated G93A Tg rats than in vehicle-treated G93A Tg rats ($p = 0.002$). Histologic evaluation of the lumbar spinal cord revealed much greater numbers of phosphorylated c-Met-positive cells (which were presumed to be motor neurons because of their large size, multipolar form, and localization in the anterior horn of the spinal cord) in hrHGF-treated G93A Tg rats compared with vehicle-treated G93A Tg rats at 2 weeks after the start of administration at 129 days (Fig. 4C, D). These observations indicated that the administered hrHGF was used in the spinal cord in G93A Tg rats. Consistent with the observation that apoptosis is involved in the pathogenesis of ALS (29–32), immunohistochemical analyses indicated large numbers of cells positive for activated caspase-3 and caspase-9 in vehicle-treated rats (Fig. 4F, H), compared with little or no reactivity in hrHGF-treated rats (Fig. 4E, G). To assess the mechanisms of suppression of caspase-3 and caspase-9 activation in hrHGF-treated rats, we next examined the level of XIAP by Western blotting, as XIAP inhibits activation of these pro-caspases and its levels are decreased in ALS mice (31). Western blotting analysis revealed increased XIAP expression

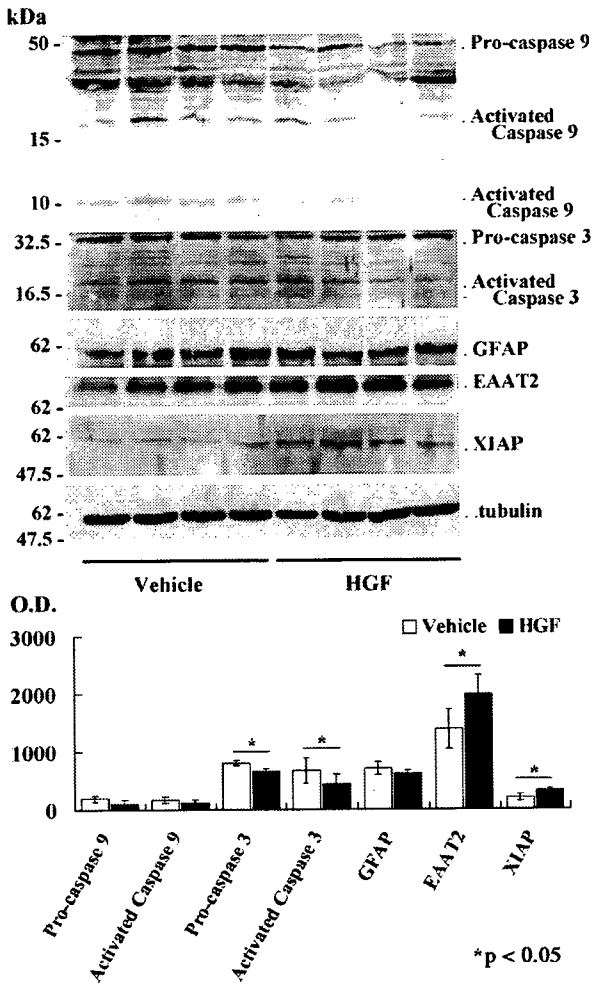

FIGURE 5. Caspase-3 and -9, glial fibrillary acidic protein (GFAP), excitatory amino acid transporter 2 (EAAT2), X-linked inhibitor of apoptosis protein (XIAP), and β-tubulin expression in the lumbar spinal cord. Western blotting of lumbar spinal cord lysates from G93A transgenic (Tg) rats treated with 100 μg of human recombinant hepatocyte growth factor (hrHGF) or vehicle for 2 weeks from 115 days. Western blotting analysis revealed increased levels of EAAT2 and XIAP expression in the spinal cords of hrHGF-treated G93A Tg rats compared with vehicle-treated G93A Tg rats (XIAP, $p = 0.0099$; EAAT2, $p = 0.0417$; $n = 4$). On the other hand, activated caspase-3 and -9 expression levels were decreased in hrHGF-treated G93A Tg rats. There were significant differences in caspase-3 expression between hrHGF- and vehicle-treated G93A Tg rats (pro-caspase-3, $p = 0.0031$; activated caspase-3, 0.0154; $n = 4$). GFAP expression was equivalent in both groups.

in the spinal cord of G93A Tg rats, and the increase in hrHGF-treated rats was only 60% of that in vehicle-treated G93A Tg rats. On the other hand, activated caspase-3 and 9 levels were decreased in hrHGF-treated G93A Tg rats ($p = 0.0154$ and $p = 0.2364$, 75% and 69% of vehicle-treated G93A Tg rats, respectively). These were all considered to be effects of HGF on motor neurons. Finally, we examined whether HGF improves the function of other cell types, such as astrocytes. There was a 60% increase in glial-specific glutamate transporter (EAAT2) in hrHGF-treated rats compared with vehicle-treated controls, although there was little difference in GFAP expression levels between the 2 groups (Fig. 5).

DISCUSSION

In this study, we demonstrated dose-dependent effects of hrHGF on motor neurons in the G93A Tg rat model of ALS, with administration starting at 100 days. Furthermore, we showed that hrHGF retards disease progression in this animal model treated from 115 days at the time of disease onset. There have been many studies of possible treatments in a mouse model of ALS (33, 34), but few agents have been shown to prolong survival with administration starting around disease onset (6–12). In this study, recombinant hrHGF retarded disease development even with administration beginning around the age onset of paralysis. Here, we showed the therapeutic effects of intrathecal delivery of a neurotrophic factor as a protein, rather than a transgene, on ALS beginning at the onset of paralysis. The average survival period of hrHGF-treated rats was 62.7% longer than that of vehicle-treated controls, comparable with the improved survival obtained by viral delivery of insulin-like growth factor-1 (6). We defined the appearance of paralysis as disease onset, although this is not a sensitive indicator and appears later than the decrease in activity (10). However, the appearance of paralysis is a clinically relevant marker of disease onset because it is closer to the state at which patients will be diagnosed with the disease.

We confirmed elevation of the human HGF concentration in the lumbar cords of hrHGF-treated G93A Tg rats using a specific sandwich immunoassay. Histologic evaluation of the lumbar spinal cord revealed greater numbers of phosphorylated c-Met-positive motor neurons in hrHGF-treated G93A Tg rats. This finding suggested that HGF receptors of motor neurons were activated well by administered hrHGF (35). These observations indicated that the administered hrHGF penetrated into the spinal cord and was utilized in the motor neurons of spinal cord. Previous studies demonstrated that many trophic factors have protective effects on motor neurons. In human trials of neurotrophic factors, such as brain-derived neurotrophic factors, glial cell line-derived neurotrophic factor, and insulin-like growth factor-1, the delivery (accessibility) of the protein to the motor neurons and glia in the spinal cord has been argued to be essential. Our results confirmed that chronic intrathecal administration with implanted infusion pumps supplied appropriate therapeutic doses to spinal cord motor neurons.

The HGF concentrations in cerebrospinal fluid are increased in many neurologic disorders, including ALS (26). In G93A Tg rats, the level of endogenous HGF in the spinal cord showed significantly greater elevation when the pathologic changes began in the spinal cord and increased with progression of the disease compared with the level of endogenous HGF in the spinal cord of non-Tg rats. After onset, the level of endogenous HGF almost doubled relative to that in non-Tg rats (Fig. 1A). These results were compatible to observations in patients with sporadic as well as familial ALS (36, 37). The level of c-met RNA expression in the lumbar cord of G93A rats increased to 155% of the normal level from before onset, and this elevated expression was retained after onset of disease (Fig. 1B). Kato et al (36) demonstrated that autocrine and paracrine trophic support of the HGF-c-met system contributes to attenuation of the degeneration of residual spinal cord motor neurons in ALS, whereas disruption of the HGF-c-met system at an advanced stage of disease accelerates cellular degeneration (37). Administration of hrHGF delayed the pathologic changes in G93A Tg rats. This effect of HGF may be due to replenishment of the relative insufficiency of HGF in G93A Tg rats in the present study.

Consistent with the findings that apoptosis is involved in ALS (29–31), large numbers of cells immunopositive for activated caspase-3 and -9 were observed in vehicle-treated animals in contrast to little or no reactivity in hrHGF-treated rats. This result was verified by quantitative Western blotting analysis, which indicated that HGF could block caspase activation of apoptosis. Caspase-3 and -9 are the main factors involved in execution of the caspase cascade. The survival-prolonging effect of HGF may be explained by suppression of induction and activation of caspase-9, as this enzyme is involved in determining disease duration (31). These observations suggest that the mechanism of the therapeutic effect of HGF in G93A Tg rats includes inhibition of the caspase cascade or of the cell death mechanism preceding the caspase cascade. In addition, EAAT2 and XIAP expression levels were increased in the hrHGF-treated group compared with vehicle-treated controls, indicating that HGF affected not only motor neurons via inhibition of the caspase cascade but also other cell types, such as astrocytes, which support motor neurons by maintaining or reinforcing internal cell protective functions, such as EAAT2 and XIAP.

Our results demonstrate pathologic improvements and retarded progression of ALS in G93A Tg rats by intrathecal administration of hrHGF from around the time of disease onset. Because HGF and c-Met are thought to be regulated in cases of not only familial but also sporadic ALS in a manner similar to the Tg mouse model of ALS (36), our findings suggest the possibility of clinical use of HGF in both familial and sporadic ALS. The results indicating the efficiency of hrHGF administration even from the onset of paralysis should prompt further clinical trials in ALS.

ACKNOWLEDGMENT

We thank Rieko Kamii for technical assistance.

REFERENCES

1. Rowland LP. Amyotrophic lateral sclerosis. Curr Opin Neurol 1994;7: 310–15
2. Mulder DW, Kurland LT, Offord KP, et al. Familial adult motor neuron disease: Amyotrophic lateral sclerosis. Neurology 1986;36:511–17

3. Rosen DR. Mutations in Cu/Zn superoxide dismutase gene are associated with familial amyotrophic lateral sclerosis. Nature 1993; 364:362
4. Deng HX, Hentati A, Tainer JA, et al. Amyotrophic lateral sclerosis and structural defects in Cu,Zn superoxide dismutase. Science 1993;261: 1047–51
5. Aoki M, Ogasawara M, Matsubara Y, et al. Mild ALS in Japan associated with novel SOD mutation. Nat Genet 1993;5:323–24
6. Kaspar BK, Llado J, Sherkat N, et al. Retrograde viral delivery of IGF-1 prolongs survival in a mouse ALS model. Science 2003;301:839–42
7. Azzouz M, Ralph GS, Storkebaum E, et al. VEGF delivery with retrogradely transported lentivector prolongs survival in a mouse ALS model. Nature 2004;429:413–17
8. Kieran D, Kalmar B, Dick JR, et al. Treatment with arimoclomol, a coinducer of heat shock proteins, delays disease progression in ALS mice. Nat Med 2004;10:402–5
9. Rothstein JD, Patel S, Regan MR, et al. β-Lactam antibiotics offer neuroprotection by increasing glutamate transporter expression. Nature 2005;433:73–77
10. Storkebaum E, Lambrechts D, Dewerchin M, et al. Treatment of motoneuron degeneration by intracerebroventricular delivery of VEGF in a rat model of ALS. Nat Neurosci 2005;8:85–92
11. Wu AS, Kiaei M, Aguirre N, et al. Iron porphyrin treatment extends survival in a transgenic animal model of amyotrophic lateral sclerosis. J Neurochem 2003;85:142–50
12. Crow JP, Calingasan NY, Chen J, et al. Manganese porphyrin given at symptom onset markedly extends survival of ALS mice. Ann Neurol 2005;58:258–65
13. Nagai M, Aoki M, Miyoshi I, et al. Rats expressing human cytosolic copper-zinc superoxide dismutase transgenes with amyotrophic lateral sclerosis: Associated mutations develop motor neuron disease. J Neurosci 2001;21:9246–54
14. Howland DS, Liu J, She Y, et al. Focal loss of the glutamate transporter EAAT2 in a transgenic rat model of SOD1 mutant-mediated amyotrophic lateral sclerosis (ALS). Proc Natl Acad Sci USA 2002;99: 1604–9
15. Ochs G, Penn RD, York M, et al. A phase I/II trial of recombinant methionyl human brain derived neurotrophic factor administered by intrathecal infusion to patients with amyotrophic lateral sclerosis Amyotroph Lateral Scler Other Motor Neuron Disord 2000;1:201–6
16. Ochs G, Giess R, Bendszus M, et al. Epi-arachnoidal drug deposit: A rare complication of intrathecal drug therapy. J Pain Symptom Manage 1999;18:229–32
17. Nakamura T, Nishizawa T, Hagiya M, et al. Molecular cloning and expression of human hepatocyte growth factor. Nature 1989;342: 440–43
18. Jung W, Castren E, Odenthal M, et al. Expression and functional interaction of hepatocyte growth factor-scatter factor and its receptor c-met in mammalian brain. J Cell Biol 1994;126:485–94
19. Matsumoto K, Nakamura T. HGF: Its organotrophic role and therapeutic potential. Ciba Found Symp 1997;212:198–211; discussion 11–14
20. Maina F, Klein R. Hepatocyte growth factor, a versatile signal for developing neurons. Nat Neurosci 1999;2:213–17
21. Ebens A, Brose K, Leonardo ED, et al. Hepatocyte growth factor/scatter factor is an axonal chemoattractant and a neurotrophic factor for spinal motor neurons. Neuron 1996;17:1157–72
22. Sun W, Funakoshi H, Nakamura T. Overexpression of HGF retards disease progression and prolongs life span in a transgenic mouse model of ALS J Neurosci 2002;22:6537–48
23. Liu KX, Kato Y, Narukawa M, et al. Importance of the liver in plasma clearance of hepatocyte growth factors in rats. Am J Physiol 1992;263: G642–49
24. Appasamy R, Tanabe M, Murase N, et al. Hepatocyte growth factor, blood clearance, organ uptake, and biliary excretion in normal and partially hepatectomized rats. Lab Invest 1993;68:270–76
25. Liu KX, Kato Y, Kino I, et al. Ligand-induced downregulation of receptor-mediated clearance of hepatocyte growth factor in rats. Am J Physiol 1998;275:E835–42
26. Funakoshi H, Nakamura T. Hepatocyte growth factor: From diagnosis to clinical applications. Clin Chim Acta 2003;327:1–23
27. Hayashi Y, Kawazoe Y, Sakamoto T, et al. Adenoviral gene transfer of hepatocyte growth factor prevents death of injured adult motoneurons after peripheral nerve avulsion. Brain Res 2006;1111:187–95
28. Grondard C, Biondi O, Armand AS, et al. Regular exercise prolongs survival in a type 2 spinal muscular atrophy model mouse. J Neurosci 2005;25:7615–22
29. Li M, Ona VO, Guegan C, et al. Functional role of caspase-1 and caspase-3 in an ALS transgenic mouse model. Science 2000;288: 335–39
30. Friedlander RM, Brown RH, Gagliardini V, et al. Inhibition of ICE slows ALS in mice. Nature 1997;388:31
31. Inoue H, Tsukita K, Iwasato T, et al. The crucial role of caspase-9 in the disease progression of a transgenic ALS mouse model. EMBO J 2003; 22:6665–74
32. Pasinelli P, Houseweart MK, Brown RH Jr. Caspase-1 and -3 are sequentially activated in motor neuron death in Cu,Zn superoxide dismutase-mediated familial amyotrophic lateral sclerosis. Proc Natl Acad Sci USA 2000;97:13901–6
33. Gurney ME, Pu H, Chiu AY, et al. Motor neuron degeneration in mice that express a human Cu,Zn superoxide dismutase mutation. Science 1994;264:1772–75
34. Gurney ME, Cutting FB, Zhai P, et al. Benefit of vitamin E, riluzole, and gabapentin in a transgenic model of familial amyotrophic lateral sclerosis. Ann Neurol 1996;39:147–57
35. Machide M, Hashigasako A, Matsumoto K, et al. Contact inhibition of hepatocyte growth regulated by functional association of the c-Met/ hepatocyte growth factor receptor and LAR protein-tyrosine phosphatase. J Biol Chem 2006;281:8765–72
36. Kato S, Funakoshi H, Nakamura T, et al. Expression of hepatocyte growth factor and c-Met in the anterior horn cells of the spinal cord in the patients with amyotrophic lateral sclerosis (ALS): Immunohistochemical studies on sporadic ALS and familial ALS with superoxide dismutase 1 gene mutation. Acta Neuropathol (Berl) 2003;106:112–20
37. Jiang YM, Yamamoto M, Kobayashi Y, et al. Gene expression profile of spinal motor neurons in sporadic amyotrophic lateral sclerosis. Ann Neurol 2005;57:236–51

BRAIN RESEARCH 1167 (2007) 112–117

available at www.sciencedirect.com

ScienceDirect

www.elsevier.com/locate/brainres

BRAIN RESEARCH

Research Report

Increased autophagy in transgenic mice with a *G93A* mutant *SOD1* gene

*Nobutoshi Morimoto, Makiko Nagai, Yasuyuki Ohta, Kazunori Miyazaki, Tomoko Kurata, Mizuki Morimoto, Tetsuro Murakami, Yasushi Takehisa, Yoshio Ikeda, Tatsushi Kamiya, Koji Abe**

Department of Neurology, Graduate School of Medicine, Dentistry and Pharmaceutical Sciences, Okayama University, 2-5-1 Shikata-cho, Okayama 700-8558, Japan

ARTICLE INFO

Article history:
Accepted 3 June 2007
Available online 7 July 2007

Keywords:
Autophagy
LC3
mTOR
Spinal cord
G93A
ALS

ABSTRACT

Autophagy, like the ubiquitin–proteasome system, is considered to play an important role in preventing the accumulation of abnormal proteins. Rat microtubule-associated protein 1 light chain 3 (LC3) is important for autophagy, and the conversion from LC3-I into LC3-II is accepted as a simple method for monitoring autophagy. We examined a SOD1G93A transgenic mouse model for amyotrophic lateral sclerosis (ALS) to consider a possible relationship between autophagy and ALS. In our study we analyzed LC3 and mammalian target of rapamycin (mTOR), a suppressor of autophagy, by immunoassays. The level of LC3-II, which is known to be correlated with the extent of autophagosome formation, was increased in SOD1G93A transgenic mice at symptomatic stage compared with non-transgenic or human wild-type SOD1 transgenic animals. Moreover, the ratio of phosphorylated mTOR/Ser^{2448} immunopositive motor neurons to total motor neurons was decreased in SOD1G93A-Tg mice. The present data show the possibility of increased autophagy in an animal model for ALS. And autophagy may be partially regulated by an mTOR signaling pathway in these animals.

1. Introduction

In every eukaryotic cell, there are two main systems for the degradation of cytoplasmic protein; the ubiquitin–proteasome system (Ciechanover, 2006) and autophagy (Yorimitsu and Klionsky, 2005). Macroautophagy (hereafter referred to as autophagy) is considered to be the main pathway among several subtypes of autophagy. During the process of autophagy, small cytoplasmic proteins are sequestered by autophagosomes and then degraded upon fusion with lysosomes (Baba et al., 1994). In contrast to the ubiquitin–proteasome system, which accounts for most of the selective intracellular protein degradation, autophagy is less selective (Klionsky, 2005; Levine and Klionsky, 2004). Recently, 27 autophagy-related (ATG) genes were identified whose products appear to be related to the autophagy process: these genes were characterized in yeast (Klionsky et al., 2003; Yorimitsu and Klionsky, 2005). It was found that the molecular basis of autophagy may well be highly conserved from yeast to humans (Levine and Klionsky, 2004; Reggiori and Klionsky, 2002). For example, rat microtubule-associated protein 1 light chain 3 (LC3), a mammalian homologue of Atg8 plays a critical

* *Corresponding author.* Department of Neurology, Graduate School of Medicine, Dentistry and Pharmaceutical Sciences, Okayama University, 2-5-1 Shikata-cho, Okayama 700-8558, Japan. Fax: +81 86 235 7368.
E-mail address: morinobu@cc.okayama-u.ac.jp (K. Abe).

0006-8993/$ – see front matter © 2007 Elsevier B.V. All rights reserved.
doi:10.1016/j.brainres.2007.06.045

role in the formation of autophagosomes (Kirisako et al., 1999). Recently, the study of mice deficient for autophagy-related 5 (Atg5) or autophagy-related 7 (Atg7), specifically in neurons, suggested that the continuous clearance of diffuse cytosolic proteins through basal autophagy is important to prevent the accumulation of abnormal proteins, which can disrupt neural function and ultimately lead to neurodegeneration (Hara et al., 2006; Komatsu et al., 2006; Rubinsztein, 2006).

Amyotrophic lateral sclerosis (ALS) is a neurodegenerative disease caused by a selective loss of motor neurons, with 10% of ALS cases being familial. Dominant missense mutations in the gene that encodes the Cu/Zn superoxide dismutase, SOD1, are responsible for 20% of familial ALS (fALS) cases. It has been well established that mutant SOD1-mediated toxicity is caused by a gain of toxic function rather than the loss of SOD1 activity (Reaume et al., 1996). Kabuta and colleagues reported that autophagy reduced mutant SOD1-mediated toxicity and that induction of autophagy decreased mutant SOD1 protein levels: these authors proposed that the contribution of autophagy to mutant SOD1 degradation was comparable to that of proteasome pathway (Kabuta et al., 2006).

Although it is believed that a deficiency in autophagy causes neurodegeneration (Hara et al., 2006; Komatsu et al., 2006; Rubinsztein, 2006) and that autophagy plays a protective role against neurodegeneration (Berger et al., 2006; Iwata et al., 2005; Kabuta et al., 2006; Ravikumar et al., 2004, 2006; Webb et al., 2003), there have been no reports investigating autophagy in an *in vivo* model of ALS. Therefore, we examined autophagy in SOD1G93A transgenic mice to consider a possible relationship between autophagy and ALS.

2. Results

2.1. *Immunohistochemical analysis of LC3*

Immunohistochemical analysis showed that LC3 was expressed mainly in neurons of the spinal cords in non-transgenic mice (non-Tg) (Fig. 1A, C) and transgenic mice expressing the G93A mutant human SOD1 (Tg) (Fig. 1B, D), with similar staining densities. Despite the magnification, it was difficult to detect the autophagosome. Double-labeling immunofluorescent analysis of spinal cord sections with an antibody to LC3 (Fig. 1E) and another antibody (SMI-32) against neurofilament protein (Fig. 1F) showed that LC3 existed in motor neurons in both Tg and non-Tg mice (Fig. 1G).

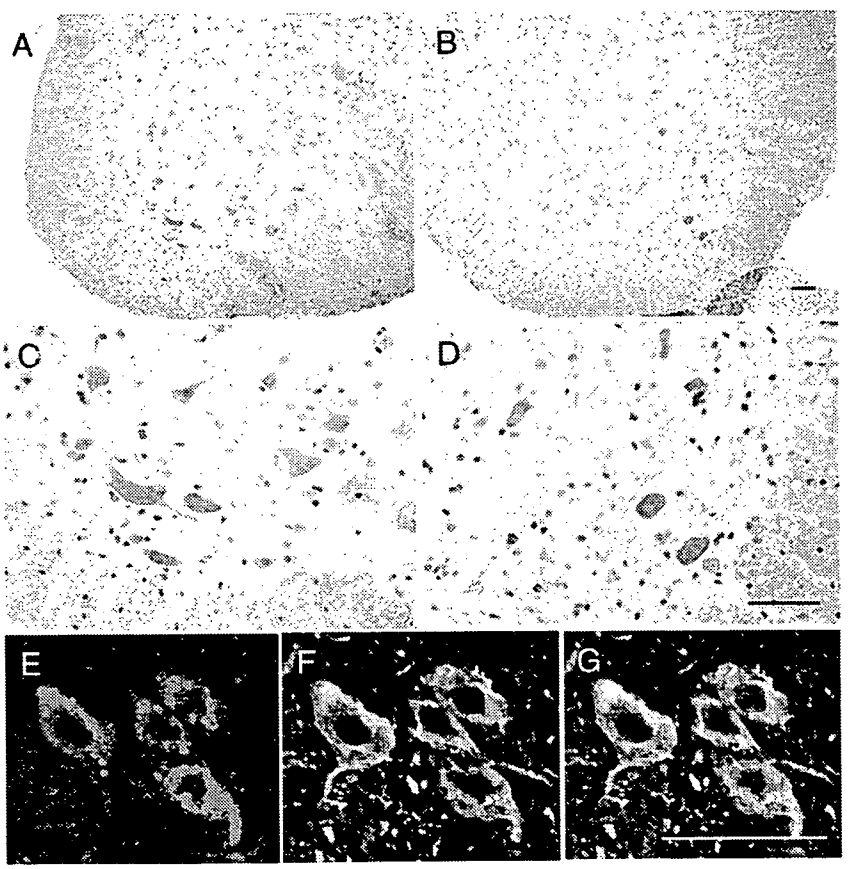

Fig. 1 – Photomicrographs of spinal cord sections from 19W SOD1G93A-Tg and non-Tg mice labeled with an antibody to LC3 and counterstained with hematoxylin–eosin. Note the LC3 expression in spinal motor neurons both of Tg mice (B, D) and non-Tg littermates (A, C). Double-labeling immunofluorescence analysis of spinal cord sections from SOD1G93A-Tg mice shows co-localization (G) of LC3 (E) and neurofilament (labeled with the monoclonal antibody SMI-32), a marker of motor neurons (F). Scale bars: 100 μm.

2.2. *Western blot analysis for LC3-II in the spinal cord*

The amount of LC3-II (relative to β-tubulin) decreased with age in non-Tg mice: 0.58±0.11 in non-Tg 10 weeks of age (W), 0.44±0.11 in non-Tg 17W, 0.32±0.06 in non-Tg 19W, mean±standard deviation (SD). Although the difference between non-Tg 10W mice and non-Tg 19W mice was highly significant; $^{**}p<0.01$, the difference between non-Tg 10W and non-Tg 17W and the difference between non-Tg 17W and non-Tg 19W were not statistically significant. Contrary to the results in non-Tg mice, the amount of LC3-II (relative to β-tubulin) in Tg mice tended to increase with age: 0.73±0.22 in Tg 10W (presymptomatic stage), 0.76±0.23 in Tg 17W (early symptomatic stage), 0.85±0.09 in Tg 19W (end symptomatic stage). However, there was no significant difference in the level of LC3-II among Tg 10W, Tg 17W and Tg 19W mice by a multiple comparison test; $p=0.61$.

The amounts of LC3-II were higher in Tg mice than in non-Tg mice at 17W: 0.44±0.11 in non-Tg vs. 0.76±0.23 in Tg; $^{*}p<0.05$, and at 19W: 0.32±0.06 in non-Tg vs. 0.85±0.09 in Tg; $^{**}p<0.01$ (Fig. 2A, B). On the other hand, at 10W, there was no significant difference between non-Tg and Tg animals: 0.58±0.11 in non-Tg vs. 0.73±0.22 in Tg; $p=0.20$.

We examined five wild-type human SOD1 transgenic mice (WtSOD1-Tg) at 19W and confirmed that the amount of LC3-II was again higher in 19W SOD1G93A-Tg mice than in WtSOD1-Tg animals: 0.36±0.08 in WtSOD1-Tg vs. 0.85±0.09 in SOD1G93A-Tg; $^{**}p<0.01$ (Fig. 3A, B).

We also examined LC3-II in cerebellar cortex of five non-Tg 17W mice and five Tg 17W mice. There was no statistically significant difference between non-Tg and Tg mice (data not shown).

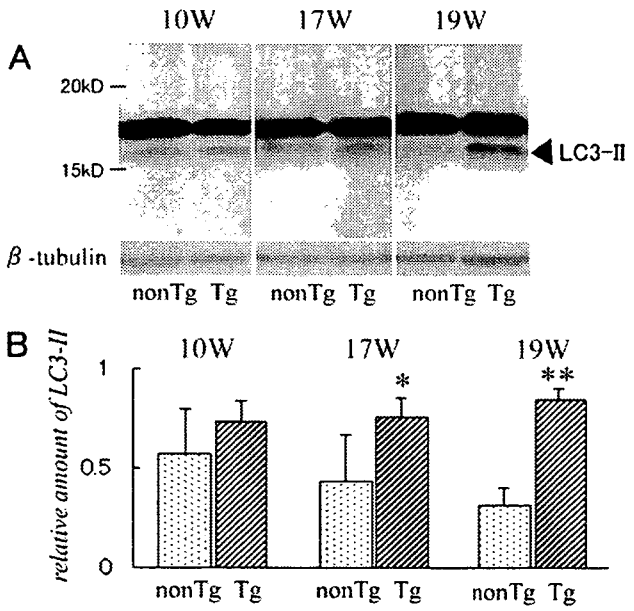

Fig. 2 – Western blot analysis of spinal cords for LC3-II protein (A) and its quantitative analysis relative to β-tubulin (B). Note the higher level of LC3-II in SOD1G93A-Tg mice than in non-Tg mice at 17W (early symptomatic stage); $n=5$, $^{*}p<0.05$ and at 19 W (end symptomatic stage); $n=5$, $^{**}p<0.01$.

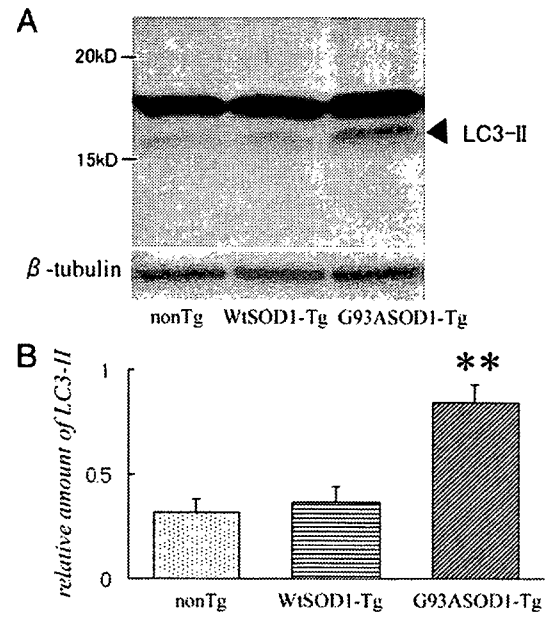

Fig. 3 – Western blot analysis of spinal cords for LC3-II protein (A) and its quantitative analysis relative to β-tubulin (B). Note the higher level of LC3-II in 19W SOD1G93A-Tg mice than in both age-matched non-Tg mice; $n=5$, $^{**}p<0.01$ and WtSOD1-Tg mice; $n=5$, $^{**}p<0.01$.

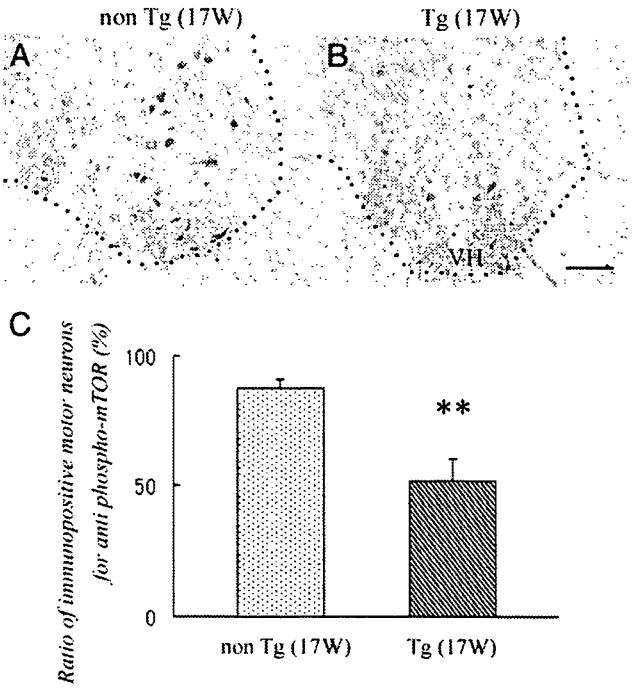

Fig. 4 – Photomicrographs of spinal cord sections labeled with antibodies to phosphorylated mTOR/Ser^{2448} (p-mTOR) (A, B). Note that the p-mTOR staining was much weaker in 17W SOD1G93A-Tg mice (B) than in age-matched non-Tg mice (A). The ratio of immunopositive motor neurons to total living motor neurons in Tg mice was significantly lower than in non-Tg mice; $n=5$, $^{**}p<0.01$, (C) at 17W. Scale bar: 100 μm. VH: ventral horn.

2.3. *Immunohistochemical analysis of phosphorylated mTOR/Ser^{2448} (p-mTOR)*

Immunohistochemical analysis of p-mTOR was performed using 17W (early symptomatic stage) mice. Immunohistochemical staining of spinal cord sections with an antibody against p-mTOR showed that the number of immunopositive motor neurons in the anterior horn areas decreased in Tg mice: 16.3±3.4/section in non-Tg vs. 4.8±0.7/section in Tg, mean±standard deviation (SD) (Fig. 4A, B). The number of living motor neurons also decreased in Tg mice: 18.6±3.7/section in non-Tg vs. 9.3±1.5/section in Tg. When the ratios of mean immunopositive motor neurons to mean living motor neurons were taken with each five Tg and five non-Tg mice, the average ratio of Tg mice was significantly lower than that of non-Tg mice: 87.6±3.6% in non-Tg vs. 52.1±8.1% in Tg; $^{**}p<0.01$ (Fig. 4C).

3. Discussion

LC3 is associated with autophagosome membranes after post-translational modifications. A C-terminal fragment of LC3 is cleaved immediately after synthesis to yield a cytosolic form called LC3-I (18 kDa). A subpopulation of LC3-I is further converted to an autophagosome-associating form, LC3-II (16 kDa). Kabeya et al. reported that the amount of LC3-II was correlated with the extent of autophagosome formation (Kabeya et al., 2000, 2004). The conversion of LC3-I into LC3-II is accepted as a simple method for monitoring autophagy (Mizushima, 2004). Consequently, we measured the extent of autophagy in fALS model mice by determination of LC3-II expression with immunoassays. Although there are more direct methods for monitoring autophagy, for example, the green fluorescent protein (GFP)-LC3 transgenic mouse (Mizushima et al., 2004) or electron microscopic analysis, our present study focused on the amount of LC3-II for simplicity. Our immunohistochemical data showed that LC3 was expressed mainly in neurons of the spinal cords both in non-Tg and Tg mice (Fig. 1). Thus, it may be considered that Western blot analysis using the whole tissue from ventral portion of the lumbar spinal cord demonstrates the extent of autophagy mainly in motor neurons that were affected by the disease.

In our study, the amount of LC3-II decreased with age in non-Tg mice (Fig. 2), consistent with reports that autophagic activity declines with age from experiments in rat (Del Roso et al., 2003). By contrast, the level of LC3-II tended to increase with age in SOD1G93A-Tg mice, and was significantly higher when compared with non-Tg littermates or WtSOD1-Tg animals (Figs. 2 and 3), suggesting that autophagosome formation increased in SOD1G93A-Tg mice. The present data show the possibility of increased autophagy in an animal model for ALS.

However, there are two ways to explain increased autophagosome formation; that autophagy is upregulated to clear the mutant proteins or that delaying the clearance of autophagosomes causes increased autophagosome formation. To confirm which hypothesis is true, assay of the lysosomal enzyme or measuring the clearance time of autophagosomes is needed.

Several genes/proteins that regulate mammalian autophagy have recently been identified. Mammalian target of rapamycin (mTOR) is a phosphatidyl inositol kinase-related kinase that negatively regulates autophagy (Schmelzle and Hall, 2000; Yorimitsu and Klionsky, 2005). It has been reported that mTOR function is activated by phosphorylation of Ser^{2448} (Nave et al., 1999; Ravikumar et al., 2003). In our study, we confirmed that the level of phosphorylated mTOR/Ser^{2448}, an activated form, decreased in SOD1G93A mutants at early symptomatic stage (Fig. 4); therefore, it is possible that autophagy is partially regulated by the mTOR intracellular signaling pathway.

There is a hypothesis that inclusion inactivates mTOR by sequestration and induces autophagy. Ravikumar and colleagues showed that mTOR was sequestered into polyglutamine-containing aggregates in cell models, transgenic mice and the brains of patients with Huntington disease. Sequestration of mTOR impairs its kinase activity and induces autophagy, a key clearance pathway for mutant huntingtin fragments. Then, induced autophagy protects against polyglutamine toxicity, as the specific mTOR inhibitor rapamycin attenuates huntingtin accumulation and cell death in cell models of Huntington disease, whereas inhibition of autophagy has the converse effect (Ravikumar et al., 2004). We considered that the appearance of mutant SOD1 aggregates in motor neurons in fALS patients and mouse models (Bruijn et al., 1997; Kato et al., 2000; Watanabe et al., 2001) suggested the existence of a similar protective pathway in fALS animals and patients.

On the other hand, recent studies have presented the evidence that insulin signal stimulates phosphorylation and activity of mTOR via Akt/PKB (Schmelzle and Hall, 2000). And Nagano et al. reported that the expressions of PI3-K and Akt/PKB were decreased in SOD1G93A-Tg mice (Nagano et al., 2002). It can also be hypothesized that the reduction of mTOR phosphorylation may be mediated by reduced PI3-K and Akt/PKB signaling in these transgenic animals.

Further research is necessary to elucidate the mechanisms of regulation for autophagy and the role of autophagy toward the motor neuron death in SOD1G93A-Tg mice.

4. Experimental procedures

4.1. *Animal model*

All experimental procedures were carried out according to the guidelines of the Animal Care and Use Committee of the Graduate School of Medicine and Dentistry of Okayama University. Transgenic mice expressing the G93A mutant human SOD1 (strain B6SJL-TGN (SOD1G93A) 1GUR^{dl}) or wild-type human SOD1 (strain C57BL/6J-TGN (SOD1) 2GUR^{dl}) were originally obtained from the Jackson Laboratory (Bar Harbor, ME; Gurney et al., 1994), then backcrossed onto a C57BL/6 background strain by mating hemizygote males with inbred C57BL/6 female mice (C57BL/6CrSlc, Nihon SLC, Sizuoka, Japan) to produce transgenic (Tg) and non-transgenic littermates (non-Tg). Our SOD1G93A-Tg mice experienced disease onset at about 15W and died at approximately 20W. In our

study, there were three experimental groups: 10W, 17W and 19W. Each group contained five Tg mice and five age-matched non-Tg mice ($n=5$).

4.2. *Primary antibodies*

The anti-LC3 antibody was obtained from Medical Biological Laboratories (#PD012). The anti-phosphorylated mTOR/Ser^{2448} antibody was obtained from Cell Signaling Technologies, and SMI-32, a marker of motor neurons, was from Berkeley Antibody Company.

4.3. *Histological analysis*

Animals were deeply anesthetized and transcardially perfused with heparinized saline, followed by 4% paraformaldehyde in 0.1 M phosphate buffer (pH 7.4). The region of the spinal cord spanning L4–5 was removed and further fixed by immersion in the same fixative for 4 h, then frozen after cryoprotection with a series of phosphate-buffered sucrose solutions of increasing concentration (10%, 15% and 20%). Transverse sections of 10 μm thickness were cut through the middle of the L4 segment on a cryostat. The LC3 antibody was used at a dilution of 1:250, and the antibody against phosphorylated mTOR/Ser^{2448} was used at 1:100. Five transverse sections from each lumbar cord were used for all histological analysis. We carried out immunohistochemical analysis by standard fluorescence methods or peroxidase labeling using the Vectastain Avidin:Biotinylated enzyme Complex (ABC) kit. We analyzed relevant negative controls without primary antibodies alongside all experiments.

4.4. *Motor neuron count*

For evaluating the percentage of immunopositive motor neurons, preserved motor neurons in the L4 segment were counted in five transverse sections from each lumbar cord stained with cresyl violet (Nissl stain). All cells in ventral horns below a lateral line across the spinal cord from the central canal were microscopically video-captured, and only cells with a diameter greater than 20 μm that showed clear nucleoli were counted by investigators who were blinded to the sample information, as described previously (Ohta et al., 2006). The average of five sections was taken as the number of living motor neurons of each animal. In addition, each mouse section was immunostained for anti-choline acetyltransferase antibody (ChAT goat antiserum; Chemicon, Temecula, CA) to confirm the results of motor neuron counting.

4.5. *Western blot analysis*

Western blot analysis was performed using the ventral portion of the lumbar spinal cord of five mice from each group. We added 0.3 mL of cold lysis buffer (50 mM Tris–HCl, pH 7.2, 10% glycerol, 250 mM NaCl, 0.1% NP-40, 2 mM EDTA and protease inhibitors) to the spinal cord tissue and homogenized it at 4 °C. The homogenate was centrifuged at 12,000 rpm at 4 °C, and the supernatant was used for Western blotting. We carried out Western blot analysis using standard techniques with an ECL Plus detection kit (GE Healthcare). The dilution of the anti-LC3 antibody was 1:500. We carried out densitometry analysis using Scion Image Beta 4.02 software and took the average of the five mice. Data obtained were analyzed by Student's t-test.

Acknowledgments

This work was partially supported by Grants-in-Aid for Scientific Research (B) 15390273 and (Hoga) 15659338 and the National Project on Protein Structural and Functional Analyses from the Ministry of Education, Science, Culture and Sports of Japan and by grants from the Ministry of Health and Welfare of Japan (to Y. Itoyama, I. Kimura, and S. Kuzuhara).

REFERENCES

Baba, M., Takeshige, K., Baba, N., Ohsumi, Y., 1994. Ultrastructural analysis of the autophagic process in yeast: detection of autophagosomes and their characterization. J. Cell Biol. 124, 903–913.

Berger, Z., Ravikumar, B., Menzies, F.M., Oroz, L.G., Underwood, B.R., Pangalos, M.N., Schmitt, I., Wullner, U., Evert, B.O., O'Kane, C.J., Rubinsztein, D.C., 2006. Rapamycin alleviates toxicity of different aggregate-prone proteins. Hum. Mol. Genet. 15, 433–442.

Bruijn, L.I., Becher, M.W., Lee, M.K., Anderson, K.L., Jenkins, N.A., Copeland, N.G., Sisodia, S.S., Rothstein, J.D., Borchelt, D.R., Price, D.L., Cleveland, D.W., 1997. ALS-linked *SOD1* mutant *G85R* mediates damage to astrocytes and promotes rapidly progressive disease with *SOD1*-containing inclusions. Neuron 18, 327–338.

Ciechanover, A., 2006. The ubiquitin proteolytic system: from a vague idea, through basic mechanisms, and onto human diseases and drug targeting. Neurology 66, S7–S19.

Del Roso, A., Vittorini, S., Cavallini, G., Donati, A., Gori, Z., Masini, M., Pollera, M., Bergamini, E., 2003. Ageing-related changes in the in vivo function of rat liver macroautophagy and proteolysis. Exp. Gerontol. 38, 519–527.

Gurney, M.E., Pu, H., Chiu, A.Y., Dal Canto, M.C., Polchow, C.Y., Alexander, D.D., Caliendo, J., Hentati, A., Kwon, Y.W., Deng, H.X., et al., 1994. Motor neuron degeneration in mice that express a human Cu,Zn superoxide dismutase mutation. Science 264, 1772–1775.

Hara, T., Nakamura, K., Matsui, M., Yamamoto, A., Nakahara, Y., Suzuki-Migishima, R., Yokoyama, M., Mishima, K., Saito, I., Okano, H., Mizushima, N., 2006. Suppression of basal autophagy in neural cells causes neurodegenerative disease in mice. Nature 441, 885–889.

Iwata, A., Christianson, J.C., Bucci, M., Ellerby, L.M., Nukina, N., Forno, L.S., Kopito, R.R., 2005. Increased susceptibility of cytoplasmic over nuclear polyglutamine aggregates to autophagic degradation. Proc. Natl. Acad. Sci. U. S. A. 102, 13135–13140.

Kabeya, Y., Mizushima, N., Ueno, T., Yamamoto, A., Kirisako, T., Noda, T., Kominami, E., Ohsumi, Y., Yoshimori, T., 2000. LC3, a mammalian homologue of yeast Apg8p, is localized in autophagosome membranes after processing. Embo J. 19, 5720–5728.

Kabeya, Y., Mizushima, N., Yamamoto, A., Oshitani-Okamoto, S., Ohsumi, Y., Yoshimori, T., 2004. LC3, GABARAP and GATE16 localize to autophagosomal membrane depending on form-II formation. J. Cell Sci. 117, 2805–2812.

Kabuta, T., Suzuki, Y., Wada, K., 2006. Degradation of amyotrophic lateral sclerosis-linked mutant Cu,Zn-superoxide dismutase proteins by macroautophagy and the proteasome. J. Biol. Chem. 281, 30524–30533.

Kato, S., Takikawa, M., Nakashima, K., Hirano, A., Cleveland, D.W., Kusaka, H., Shibata, N., Kato, M., Nakano, I., Ohama, E., 2000. New consensus research on neuropathological aspects of familial amyotrophic lateral sclerosis with superoxide dismutase 1 (SOD1) gene mutations: inclusions containing SOD1 in neurons and astrocytes. Amyotroph. Lateral Scler. Other Mot. Neuron Disord. 1, 163–184.

Kirisako, T., Baba, M., Ishihara, N., Miyazawa, K., Ohsumi, M., Yoshimori, T., Noda, T., Ohsumi, Y., 1999. Formation process of autophagosome is traced with Apg8/Aut7p in yeast. J. Cell Biol. 147, 435–446.

Klionsky, D.J., 2005. The molecular machinery of autophagy: unanswered questions. J. Cell Sci. 118, 7–18.

Klionsky, D.J., Cregg, J.M., Dunn Jr., W.A., Emr, S.D., Sakai, Y., Sandoval, I.V., Sibirny, A., Subramani, S., Thumm, M., Veenhuis, M., Ohsumi, Y., 2003. A unified nomenclature for yeast autophagy-related genes. Dev. Cell 5, 539–545.

Komatsu, M., Waguri, S., Chiba, T., Murata, S., Iwata, J., Tanida, I., Ueno, T., Koike, M., Uchiyama, Y., Kominami, E., Tanaka, K., 2006. Loss of autophagy in the central nervous system causes neurodegeneration in mice. Nature 441, 880–884.

Levine, B., Klionsky, D.J., 2004. Development by self-digestion: molecular mechanisms and biological functions of autophagy. Dev. Cell 6, 463–477.

Mizushima, N., 2004. Methods for monitoring autophagy. Int. J. Biochem. Cell Biol. 36, 2491–2502.

Mizushima, N., Yamamoto, A., Matsui, M., Yoshimori, T., Ohsumi, Y., 2004. In vivo analysis of autophagy in response to nutrient starvation using transgenic mice expressing a fluorescent autophagosome marker. Mol. Biol. Cell 15, 1101–1111.

Nagano, I., Murakami, T., Manabe, Y., Abe, K., 2002. Early decrease of survival factors and DNA repair enzyme in spinal motor neurons of presymptomatic transgenic mice that express a mutant SOD1 gene. Life Sci. 72, 541–548.

Nave, B.T., Ouwens, M., Withers, D.J., Alessi, D.R., Shepherd, P.R., 1999. Mammalian target of rapamycin is a direct target for protein kinase B: identification of a convergence point for opposing effects of insulin and amino-acid deficiency on protein translation. Biochem. J. 344 (Pt 2), 427–431.

Ohta, Y., Nagai, M., Nagata, T., Murakami, T., Nagano, I., Narai, H., Kurata, T., Shiote, M., Shoji, M., Abe, K., 2006. Intrathecal injection of epidermal growth factor and fibroblast growth factor 2 promotes proliferation of neural precursor cells in the spinal cords of mice with mutant human SOD1 gene. J. Neurosci. Res. 84, 980–992.

Ravikumar, B., Stewart, A., Kita, H., Kato, K., Duden, R., Rubinsztein, D.C., 2003. Raised intracellular glucose concentrations reduce aggregation and cell death caused by mutant huntingtin exon 1 by decreasing mTOR phosphorylation and inducing autophagy. Hum. Mol. Genet. 12, 985–994.

Ravikumar, B., Vacher, C., Berger, Z., Davies, J.E., Luo, S., Oroz, L.G., Scaravilli, F., Easton, D.F., Duden, R., O'Kane, C.J., Rubinsztein, D.C., 2004. Inhibition of mTOR induces autophagy and reduces toxicity of polyglutamine expansions in fly and mouse models of Huntington disease. Nat. Genet. 36, 585–595.

Ravikumar, B., Berger, Z., Vacher, C., O'Kane, C.J., Rubinsztein, D.C., 2006. Rapamycin pre-treatment protects against apoptosis. Hum. Mol. Genet. 15, 1209–1216.

Reaume, A.G., Elliott, J.L., Hoffman, E.K., Kowall, N.W., Ferrante, R.J., Siwek, D.F., Wilcox, H.M., Flood, D.G., Beal, M.F., Brown Jr., R.H., Scott, R.W., Snider, W.D., 1996. Motor neurons in Cu/Zn superoxide dismutase-deficient mice develop normally but exhibit enhanced cell death after axonal injury. Nat. Genet. 13, 43–47.

Reggiori, F., Klionsky, D.J., 2002. Autophagy in the eukaryotic cell. Eukaryot. Cell 1, 11–21.

Rubinsztein, D.C., 2006. The roles of intracellular protein-degradation pathways in neurodegeneration. Nature 443, 780–786.

Schmelzle, T., Hall, M.N., 2000. TOR, a central controller of cell growth. Cell 103, 253–262.

Watanabe, M., Dykes-Hoberg, M., Culotta, V.C., Price, D.L., Wong, P.C., Rothstein, J.D., 2001. Histological evidence of protein aggregation in mutant SOD1 transgenic mice and in amyotrophic lateral sclerosis neural tissues. Neurobiol. Dis. 8, 933–941.

Webb, J.L., Ravikumar, B., Atkins, J., Skepper, J.N., Rubinsztein, D.C., 2003. Alpha-Synuclein is degraded by both autophagy and the proteasome. J. Biol. Chem. 278, 25009–25013.

Yorimitsu, T., Klionsky, D.J., 2005. Autophagy: molecular machinery for self-eating. Cell Death Differ. 12 (Suppl 2), 1542–1552.

Acta Neuropathol (2008) 115:97–114
DOI 10.1007/s00401-007-0308-4

REVIEW

Amyotrophic lateral sclerosis models and human neuropathology: similarities and differences

Shinsuke Kato

Received: 29 June 2007 / Revised: 27 September 2007 / Accepted: 29 September 2007 / Published online: 17 November 2007

Abstract Amyotrophic lateral sclerosis (ALS) is a progressive neurodegenerative disease that primarily involves the motor neuron system. The author initially summarizes the principal features of human ALS neuropathology, and subsequently describes in detail ALS animal models mainly from the viewpoint of pathological similarities and differences. ALS animal models in this review include strains of rodents that are transgenic for superoxide dismutase 1 (SOD1), ALS2 knockout mice, and mice that are transgenic for cytoskeletal abnormalities. Although the neuropathological results obtained from human ALS autopsy cases are valuable and important, almost all of such cases represent only the terminal stage. This makes it difficult to clarify how and why ALS motor neurons are impaired at each clinical stage from disease onset to death, and as a consequence, human autopsy cases alone yield little insight into potential therapies for ALS. Although ALS animal models cannot replicate human ALS, in order to compensate for the shortcomings of studies using human ALS autopsy samples, researchers must inevitably rely on ALS animal models that can yield very important information for clarifying the pathogenesis of ALS in humans and for the establishment of reliable therapy. Of course, human ALS and all ALS animal models share one most important similarity in that both exhibit motor neuron degeneration/death. This important point of similarity has shed much light on the pathomechanisms of the motor neuron degeneration/death at the cellular and molecular levels that would not have been appreciated if only human ALS autopsy samples had been available. On the basis of the aspects covered in this review, it can be concluded that ALS animal models can yield very important information for clarifying the pathogenesis of ALS in humans and for the establishment of reliable therapy only in combination with detailed neuropathological data obtained from human ALS autopsy cases.

Keywords Amyotrophic lateral sclerosis · Animal models · Superoxide dismutase 1 · Transgenic rodents · Human pathology

S. Kato (✉)
Department of Neuropathology,
Institute of Neurological Sciences, Faculty of Medicine,
Tottori University, Nishi-cho 36-1, Yonago 683-8504, Japan
e-mail: kato@grape.med.tottori-u.ac.jp

Introduction

Amyotrophic lateral sclerosis (ALS) in humans is a progressive disease characterized by degeneration of both upper and lower motor neurons. Upper motor neurons are located mainly in layer V of the motor cortex, and are known as Betz cells, which are giant cells approximately 60–120 μm in diameter. Cytoarchitecturally, the axons of the upper motor neurons connect directly with the lower motor neurons located in the motor nuclei of the brainstem and the anterior horn of the spinal cord. The axons of the lower motor neurons project mainly to skeletal muscles. Although an essential pathological feature of ALS is motor neuron loss, affected motor neurons often contain characteristic inclusions in the perikarya, dendrites and axons. The concept of "ALS" has been widely debated for over 130 years since Charcot first introduced the term "la sclérose latérale amyotrophique" in 1874 [15]. Currently, in the era of advanced genetics, the molecular bases and mechanisms of ALS are now known to be very complex, thus explaining the different phenotypes of ALS. Therefore, ALS is considered to be a type of syndrome rather than a single disease entity.

Human pathologists are entirely dependent on human ALS autopsy samples in order to acquire a more definitive understanding of the etiology and pathogenesis of ALS motor neuron death. As almost all ALS autopsy samples are obtained from patients at the terminal stage, it is difficult to clarify how and why ALS motor neurons are impaired at each clinical stage from disease onset to death. Therefore, analyses of ALS autopsy samples alone is not sufficient to lead to possible therapies for ALS. Under these circumstances, many researchers including pathologists have come to rely on animal models of ALS in order to gain insights into both the mechanisms involved in motor neuron death and possible therapeutic approaches. Inevitably, these ALS animal models have different characteristics, because even human ALS, which is the prototype for these models, is not a single disease. On the basis of the aspects covered in this review, however, the author wish to emphasize that ALS animal models can yield very important information for clarifying the pathogenesis of ALS in humans only in combination with detailed neuropathological data obtained from human ALS autopsy cases.

Human ALS neuropathology

Sporadic ALS (SALS)

Human ALS is classified into two major subtypes: sporadic ALS (SALS) and familial ALS (FALS). In SALS, the degenerative change is mainly restricted to the motor neuron system, except for the oculomotor, trochlear and abducens nuclei controlling eye movements, as well as Onufrowicz's nucleus which functions in fecal and urinary continence. Upper motor neurons such as the Betz cells in the motor cortex are also affected. Degeneration of the corticospinal tracts in the anterior and lateral columns of the spinal cord are particularly evident. Especially, the corticospinal tract degeneration is most evident in the lower spinal cord segment, supporting the hypothesis of a dying back degeneration of axons. In the degenerated primary motor tracts, there is loss of large myelinated fibers in association with variable astrocytic gliosis. Destruction of these fibers is usually associated with the appearance of lipid-laden macrophages.

An essential histopathological feature of SALS is loss of both upper and lower motor neurons, especially large anterior horn cells throughout the length of the spinal cord. In addition, striated muscles demonstrate denervation atrophy, i.e., neurogenic muscle atrophy. The surviving motor neurons often show histopathological features including cytoplasmic shrinkage and lipofuscin granules. The cytopathology of the affected motor neurons in SALS is characterized by the following two important intracytoplasmic inclusions.

Bunina bodies

Bunina bodies are small eosinophilic granular inclusions (1–3 μm in diameter) in the anterior horn cells, appearing either singly or in a group, and sometimes arranged in small beaded chains. These Bunina bodies are observed within the cytoplasm or dendrites (Fig. 1a), but they have not been found within the axoplasm. Bunina bodies stain bright red with hematoxylin and eosin (H&E) staining, deep blue with phosphotungstic acid hematoxylin, and blue with Luxol fast blue. Immunohistochemical studies have revealed that they express only cystatin C (Fig. 1b), and do not have a variety of other immunoreactive epitopes such as ubiquitin. Ultrastructurally, Bunina bodies consist of electron-dense amorphous material that contains tubules or vesicular structures. The amorphous material frequently includes a cytoplasmic island containing neurofilaments and other micro-organelles [58].

These specific bodies were originally described by a Russian pathologist Bunina [12] in 1962 in two FALS patients belonging to two different families. After Bunina's report, Hirano immediately confirmed that these inclusion bodies were present in a number of ALS patients, including those with SALS and FALS neuropathologically identical to SALS, as well as Guamanian ALS [41]. Although not all ALS patients necessarily have Bunina bodies histologically, Bunina bodies themselves are currently considered a specific histopathological hallmark of ALS. Broadly speaking, Bunina bodies can be observed in SALS, frontotemporal lobar degeneration with motor neuron disease (FTLD-MND; terminologically identical to ALS with dementia, ALSD), mutant SOD1-unlinked FALS that is neuropathologically identical to SALS, and Guamanian ALS. However, there have been no reports that Bunina bodies are present in SOD1-mutated FALS (Table 1) or transgenic rodents with mutant SOD1.

Skein-like inclusions (SLIs) and round hyaline inclusions (RHIs)

The SLIs are intracytoplasmic filamentous structures [58] that are frequently encountered in preparations immunostained for ubiquitin, although in H&E preparations they are hardly visible or sometimes detected as faintly eosinophilic structures. SLIs form essential aggregates of thread-like structures. In more aggregated forms, SLIs show dense collections of filaments, in which the SLIs appear as spherical structures. RHIs are pale eosinophilic inclusions with halos in the remaining anterior horn cells in H&E preparations [57]. Sometimes, they lack halos and have irregular margins associated with filamentous structures similar to SLIs. Immunohistochemically, SLIs and RHIs are positive for ubiquitin, but negative for phosphorylated

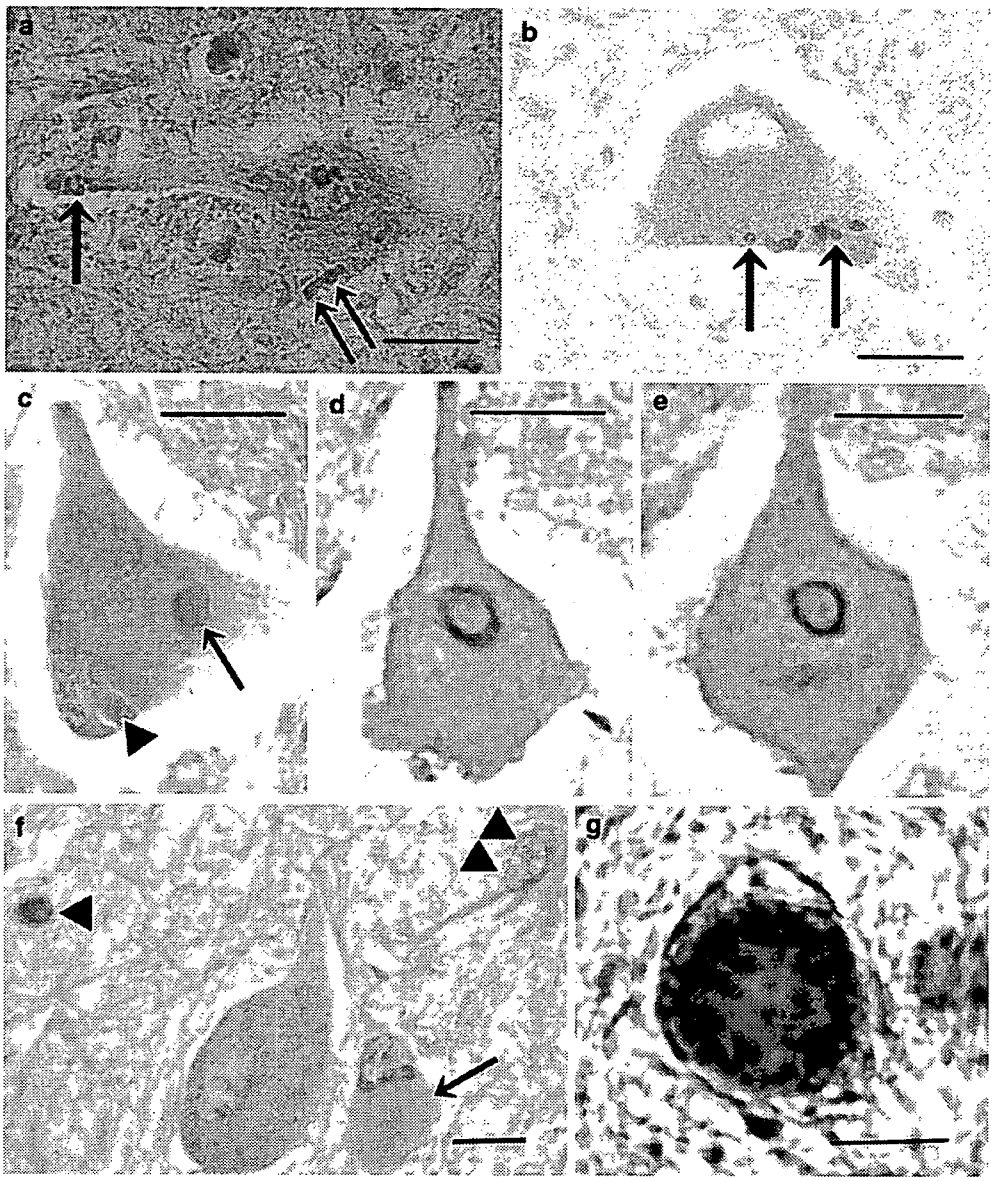

Fig. 1 Neuropathological findings of human ALS. **a**, **b** Light micrographs of Bunina bodies. **a** Bunina bodies in an anterior horn cell of an SALS patient. Bunina bodies are small eosinophilic inclusions (approximately 1–3 μm in diameter) and staining bright red with H&E. Bunina bodies are observed within the cytoplasm (*double arrows*), being arranged in a chain-like formation. In addition, Bunina bodies are also seen within the dendrites (*arrow*), appearing as a cluster. H&E. **b** Cystatin C immunostaining. Bunina bodies are positive for cystatin C (*double arrows*). A Bunina body (indicated by the *center arrow*) appears as a round structure with central-lucent core, which corresponds to a cytoplasmic island containing neurofilaments and other microorgans at the ultrastructural level. **c–e** Light micrographs of neuronal Lewy-body-like hyaline inclusions (LBHIs). **c** A round LBHI (*arrow*) is observed in the cytoplasm of the anterior horn cell. This round LBHI is composed of eosinophilic core with paler peripheral halo. A small ill-defined LBHI (*arrowhead*) is also seen in the cytoplasm of the anterior horn cell, and consists of obscure slightly eosinophilic materials. H&E. **d, e** Serial sections of a neuronal LBHI in a spinal anterior horn cell immunostained with the antibodies against SOD1 (**d**) and ubiquitin (**e**). An intraneuronal LBHI is clearly labeled by the antibodies to SOD1 and ubiquitin. The immunoreactivity for both SOD1 and ubiquitin is almost restricted to the halo of the LBHI. **f** Light micrograph of an astrocytic hyaline inclusion (Ast-HI) in the spinal cord anterior horn. The Ast-HI (*arrow*) is round and eosinophilic. The astrocyte-bearing the Ast-HI is morphologically different from the adjacent neuron. The nucleus of the cell bearing the Ast-HI resembles that of a reactive astrocyte (*double arrowheads*) and not the nucleus of an oligodendrocyte (*arrowhead*). H&E. **g** A neurofilamentous conglomerate inclusion showing intense immunohistochemical positivity for phosphorylated neurofilament protein. Scale bar **a** (also for **b–e**, **g**) 30 μm, Scale bar **f** 10 μm

(p) neurofilament protein (NFP; pNFP) and SOD1 [58]. Ultrastructurally, the essential abnormal filaments of the SLIs range in width from approximately 15 nm in the naked parts without granules to about 20 nm in parts with fuzzy granules (i.e., fibrils with granules); these fibrils with granules often form bundles. In more aggregated

Table 1 Summary of main neuropathological findings in autopsied patients with familial amyotrophic lateral sclerosis (FALS) with characteristic mutations of superoxide dismutase 1 (SOD1)

SOD1 mutation	Number of patients	Neuronal inclusion	SOD1 aggregation	Bunina body	Corticospinal tract involvement	Posterior column involvement	References
A4V	3	LBHI	+	−	+(slight)	+	[89]
	5	ICI	ND	ND	±(mild)	+(asymmetry)	[18]
A4T	1	LBHI	+	−	+(mild)	+	[92]
G37R	1	LBHI	+	−	+	+	[46]
H43R	1	LBHI	+	−	+	+	[67]
H46R	1	LBHI	+	−	+(very mild)	+(very mild)	[76]
H48Q	1	LBHI&SLI	−	−	+(mild)	minimal	[88]
E100G	1	SLI	−	ND	+	+	[44]
D101N	2	ICHI	ND	ND	−	−	[14]
D101Y	1	LBHI	+	−	+(very mild)	−	[94]
L106V	2	LBHI	+	−	+	+	(Unpublished data from author)
C111Y	1	LBHI	+	−	+	Minimal	[32]
I113T	1	NFT (Brain and brain stem)	ND	ND	+	−	[78]
	1	ICAI	ND	ND	−	ND	[85]
	1	ICAI	+	−	ND	ND	[60]
	1	HC	ND	ND	+	+	[45]
	1	NFCI	−	−	+(slight)	+	[51]
L126S	1	LBHI	+	−	+	+	[93]
2-bp del	2	LBHI	+	−	+(slight/marked)	+	[53]
(L126delTT)	1	LBHI	+	−	+	−	[50]
C146R	2	LBHI	+	−	+(slight)	+	[71]
Wild type	2	SLI/RHI	−	+	+	−	(Unpublished data from author)

As controls, FALS siblings with wild-type SOD1 are also tabulated in the bottom row

+, present; −, absent

ND not described; *LBHI* Lewy-body-like hyaline inclusion; *ICI* intracytoplasmic inclusion; *SLI* skein-like inclusion; *RHI* round hyaline inclusion; *ICHI* intracytoplasmic hyaline inclusion; *NFT* neurofibrillary tangle (straight filament); *ICAI* intracytoplasmic argyrophilic inclusion (neurofilament accumulation); *HC* hyaline conglomerate (with neurofilament epitope); *NFCI* neurofilamentous conglomerate inclusion; *bp*, base pair; *del* deletion

forms, SLIs that appear to be spherical structures are composed of many bundles of these fibrils with granules [58]. Ultrastructurally, the essential abnormal filaments of the RHIs range in width from approximately 15 nm in the naked parts without granules to about 20 nm in the parts with fuzzy granules (fibrils with granules), being very similar to the fibrils with granules in SLIs [58]. As a whole, RHIs form spherical aggregates without a limiting membrane, and a hypothesis that SLIs evolve to RHIs has even been proposed [58]. Unlike Lewy body-like hyaline inclusions (LBHIs) in mutant SOD1-linked motor neurons, although RHIs are similar to LBHIs in H&E preparations, RHIs are negative for SOD1 [58]. Simply and clearly to state, SLIs/RHIs are ultrastructurally composed of 15–20-nm fibrils with granules, and LBHIs comprised of 15–25-nm granule-coated fibrils with SOD1 epitope [58] (see "Neuronal LBHIs and Ast-HIs").

Familial ALS (FALS)

The FALS accounts for approximately 5–10% of all cases of ALS, and is histopathologically subclassified into two types. One type of FALS is neuropathologically identical to SALS, and frequently contains Bunina bodies. On the basis of the author's observations of two mutant SOD1-unlinked siblings with FALS, this mutant SOD1-non-linked FALS type has similar neuropathological features including Bunina bodies and SLIs/RHIs (Table 1). It is likely that the inclusion bodies originally described by Bunina (Bunina bodies) would have been present in this FALS type. The other form of FALS is that showing posterior column involvement. In addition to the pathological features of SALS, this form also shows degeneration of the middle zone of the posterior column, Clarke nuclei and posterior spinocerebellar tracts. In 1967, Hirano et al. [42] reported

the presence of Lewy body-like hyaline inclusions (LBHIs) in the anterior horn cells throughout the spinal cord in this type of FALS (Fig. 1c). This led to the establishment of this entity as FALS with posterior column involvement. In H&E preparations, neuronal LBHIs show an eosinophilic core with a paler peripheral halo, and their name is derived from their H&E staining features, which resemble those of Lewy bodies in patients with Parkinson's disease.

To date, more than 100 different mutations within all exons of the SOD1 gene and its introns have been identified as being involved in the development of chromosome 21q-linked FALS. These SOD1 gene mutations are present in about 20% of FALS patients. SOD1-mutated FALS shows a variety of clinical phenotypes according to which type of SOD1 gene mutation is responsible: the disease onset and duration are reported to be closely linked to the type of the SOD1 mutation (Fig. 2), i.e., as Fig. 2 demonstrates, FALS with mutant G93A SOD1 shows rapid disease progression with severe neurological symptoms (about 1 year to at most 4 years), while FALS with mutant H46R SOD1 has a very long disease duration with mild neurological signs (11–24 years). From the viewpoint of only the copy number of the mutant SOD1 gene, almost all FALS patients with heterozygosity for the mutant SOD1 gene carry only a single copy of mutant SOD1 gene, i.e., most patients with SOD1-mutated FALS have the same transgene copy number. Based on this notion, it might be expected that FALS patients with heterozygosity for the mutant SOD1 gene would exhibit a similar expression level of mutant SOD1 protein. However, the protein expression level of mutant SOD1 in FALS patients differs due to the difference in stability of the mutant SOD1 protein itself; FALS patients with unstable-type mutant SOD1 show a lower protein expression level than FALS patients with stable-type mutant SOD1 [86].

Neuropathologically, it is of note that many SOD1-mutated FALS cases are of the posterior column involvement type with neuronal LBHIs (Table 1). In addition to neuronal LBHIs, certain long-surviving FALS patients with SOD1 gene mutations show astrocytic hyaline inclusions (Ast-HIs), which were first reported by the author in 1996 [53] (Fig. 1f). Neuronal LBHIs and Ast-HIs are characteristic intracytoplasmic structures in SOD1-mutated cells. By marked contrast, Bunina bodies have not been described in mutant SOD1-linked FALS unlike mutant SOD1-unlinked FALS with Bunina bodies (Table 1).

Neuronal LBHIs and Ast-HIs

Neuronal LBHIs and Ast-HIs in SOD1-mutated FALS have strong SOD1 immunoreactivity (Fig. 1d), and both type of inclusion are strongly positive for ubiquitin (Fig. 1e). Interestingly, LBHIs/Ast-HIs contain both wild-type and mutant SOD1 protein [11]. Ultrastructurally, neuronal LBHIs, which consist of filaments and granular materials, exhibit dense cores with rough peripheral halos and lacking a limiting membrane. The filaments of these inclusions are composed of approximately 15–25-nm granule-coated fibrils in association with normal 10-nm neurofilaments [53–57]. The neurofilaments are located mainly in the periphery and rarely in the central portion. Ast-HIs appear as globular structures that are well demarcated from other cytoplasmic structures, and have no limiting membrane. Ast-HIs are composed of about 15–25-nm granule-coated fibrils with granular materials, sometimes surrounded by normal glial filaments [53–57]. The essential constituents common to both neuronal LBHIs and Ast-HIs are granule-coated fibrils, and the indirect immunogold technique shows labeling with colloidal gold particles for wild-type and mutant SOD1 only on the surface of the granule-coated fibrils: the essential common constituents of LBHIs/Ast-HIs are SOD1-positive granule-coated fibrils [57].

Another characteristic pathological feature of patients with SOD1-mutated FALS is slight or mild corticospinal tract involvement, in contrast to severe degeneration of the lower motor neurons (Table 1). In patients with FALS lacking LBHI with the I113T mutation, neurofilament pathology is an almost universal feature. Frequently, neurofilamentous conglomerate inclusions (NFCIs) are evident, while they are less common in patients with SALS (less than 5%). Although NFCIs are recognized as homogeneous, faintly eosinophilic, oval or multi-lobulated inclusions in H&E preparations, they are intensely positive for pNFP immunohistochemically (Fig. 1g). Two FALS siblings with wild-type SOD1 in the bottom row of Table 1 show Bunina bodies and SLIs/RHIs that are usually observed in SALS, and neuropathologically they showed histology that was almost identical to SALS. These two mutant SOD1-unlinked FALS siblings did not exhibit LBHIs or posterior column degeneration. Although SLIs are seen in SALS and mutant SOD1-unlinked FALS as well as FALS with H48Q and E100G, many cases of SOD1-mutated FALS do not show SLIs (Table 1).

Transgenic animal models linked to superoxide dismutase 1 (SOD1)

Main characteristics of animal models based on SOD1

It is possible to create transgenic animals (rodents) expressing the human wild-type and mutated SOD1 gene. Currently, transgenic rodents expressing human mutant SOD1 are thought to provide the most suitable animal model of human ALS. There are several lines of transgenic rodents expressing human mutant SOD1, and their main characteristics